Marine Geology 272 (2010) 26–48

Contents lists available at ScienceDirect

Marine Geology

journal homepage: www.elsevier.com/locate/margeo

Tectonic and geological framework for gas hydrates and cold seeps on the Hikurangi subduction margin, New Zealand

Philip M. Barnes [a,*], Geoffroy Lamarche [a], Joerg Bialas [b], Stuart Henrys [c], Ingo Pecher [d], Gesa L. Netzeband [b], Jens Greinert [e,1], Joshu J. Mountjoy [a,f], Katherine Pedley [f], Gareth Crutchley [g]

[a] National Institute of Water & Atmospheric Research, P.O. Box 14901, Kilbirnie, Wellington 6041, New Zealand
[b] Leibniz Institute of Marine Sciences, IFM-GEOMAR, Wischhofstr. 1-3, 24148, Kiel, Germany
[c] GNS Science, P.O. Box 30368, Lower Hutt, New Zealand
[d] Institute of Petroleum Engineering, Heriot-Watt University, Edinburgh, EH3 9HP, Scotland, UK
[e] Renard Centre of Marine Geology, University of Gent, Belgium
[f] Department of Geological Sciences, University of Canterbury, Private Bag 4800, Christchurch, New Zealand
[g] Department of Geology, University of Otago, P.O. Box 56, Dunedin 9054, New Zealand

ARTICLE INFO

Article history:
Received 2 July 2008
Received in revised form 18 February 2009
Accepted 8 March 2009
Available online 31 March 2009

Keywords:
Hikurangi
subduction
interplate décollement
thrust wedge
thrust faults
accretion
subducting seamounts
anticline
turbidites
gas hydrates
fluid seeps

ABSTRACT

The imbricated frontal wedge of the central Hikurangi subduction margin is characteristic of wide (ca. 150 km), poorly drained and over pressured, low taper (~4°) thrust systems associated with a relatively smooth subducting plate, a thick trench sedimentary sequence (~3–4 km), weak basal décollement, and moderate convergence rate (~40 mm/yr). New seismic reflection and multibeam bathymetric data are used to interpret the regional tectonic structures, and to establish the geological framework for gas hydrates and fluid seeps. We discuss the stratigraphy of the subducting and accreting sequences, characterize stratigraphically the location of the interplate décollement, and describe the deformation of the upper plate thrust wedge together with its cover sequence of Miocene to Recent shelf and slope basin sediments. We identify approximately the contact between an inner foundation of deforming Late Cretaceous and Paleogene rocks, in which widespread out-of-sequence thrusting occurs, and a 65–70 km-wide outer wedge of late Cenozoic accreted turbidites. Although part of a seamount ridge is presently subducting beneath the deformation front at the widest part of the margin, the morphology of the accretionary wedge indicates that frontal accretion there has been largely uninhibited for at least 1–2 Myr. This differs from the offshore Hawkes Bay sector of the margin to the north where a substantial seamount with up to 3 km of relief has been subducted beneath the lower margin, resulting in uplift and complex deformation of the lower slope, and a narrow (10–20 km) active frontal wedge.

Five areas with multiple fluid seep sites, referred to informally as Wairarapa, Uruti Ridge, Omakere Ridge, Rock Garden, and Builders Pencil, typically lie in 700–1200 m water depth on the crests of thrust-faulted, anticlinal ridges along the mid-slope. Uruti Ridge sites also lie in close proximity to the eastern end of a major strike-slip fault. Rock Garden sites lie directly above a subducting seamount. Structural permeability is inferred to be important at all levels of the thrust system. There is a clear relationship between the seeps and major seaward-vergent thrust faults, near the outer edge of the deforming Cretaceous and Paleogene inner foundation rocks. This indicates that thrust faults are primary fluid conduits and that poor permeability of the Cretaceous and Paleogene inner foundation focuses fluid flow to its outer edge. The sources of fluids expelling at active seep sites along the middle slope may include the inner parts of the thrust wedge and subducting sediments below the décollement. Within anticlinal ridges beneath the active seep sites there is a conspicuous break in the bottom simulating reflector (BSR), and commonly a seismically-resolvable shallow fault network through which fluids and gas percolate to the seafloor. No active fluid venting has yet been recognized over the frontal accretionary wedge, but the presence of a widespread BSR, an extensive protothrust zone (>200 km by 20 km) in the Hikurangi Trough, and two unconfirmed sites of possible previous fluid expulsion, suggest that the frontal wedge could be actively dewatering. There are presently no constraints on the relative fluid flux between the frontal wedge and the active mid-slope fluid seeps.

* Corresponding author. Tel.: +64 4 386 0372; fax: +64 4 386 2153.
E-mail address: p.barnes@niwa.co.nz (P.M. Barnes).
[1] Present address: Royal Netherlands Institute for Sea Research, P.O. Box 59, 1790 AB, Den Burg (Texel), The Netherlands.

0025-3227/$ – see front matter © 2009 Elsevier B.V. All rights reserved.
doi:10.1016/j.margeo.2009.03.012

1. Introduction

Gas hydrates and cold seeps are characteristics of many active continental margins. They reflect the migration of fluids and gas towards the seabed as a result of tectonic deformation, compaction, porosity reduction, and dewatering of the sedimentary sequence (Kvenvolden, 1993). Seafloor sites of methane rich fluid expulsion may be characterized by the presence of chemosynthetic biological communities, development of carbonate hard grounds, pockmark depressions, mud volcanism, and/or hydroacoustic flares (e.g., Kulm and Suess, 1990; Henry et al., 1990; Trehu et al., 1999; Faure et al., 2006). In subduction margins, particularly those dominated by accretion, high fluid pressures are thought to play an important mechanical role in maintaining thrust wedges (Moore and Byrne, 1987; Bryne and Fisher, 1990, Moore and Vrolijk, 1992; Bangs et al., 1999, 2004; Saffer and Bekins, 2002), and in the seismogenic cycle by producing fluctuations in frictional strength of faults (Sibson, 1992; Dixon and Moore, 2007 and papers therein). Fault zones are commonly interpreted as important conduits for the upward flow of fluid (e.g., Moore et al., 1990, 1995).

The 25 Myr old Hikurangi Margin of north eastern New Zealand epitomizes subduction systems and their tectonic complexity and variability. Lying at the southern end of the Tonga–Kermadec–Hikurangi subduction zone, the margin has formed in response to the westward subduction of the thick and bathymetrically elevated oceanic Hikurangi Plateau (Pacific Plate) beneath the Australian Plate at about 40–50 mm/yr (Fig. 1). The structural trench, referred to as the Hikurangi Trough, is shallow (c. 3000 m) compared to the deep Kermadec trench (>9000 m), and the plate interface dips at a gentle angle of about 3° for at least 100 km beneath the margin, before steepening beneath the North Island (Davey et al., 1986a; Henrys et al., 2006; Barker et al., 2009). The margin exhibits complex tectonic structure and stratigraphic evolution (e.g., Lewis and Pettinga, 1993; Collot et al., 1996; Field et al., 1997; Barnes et al., 2002; Barnes and Nicol, 2004; Henrys et al., 2006; Nicol et al., 2007). The northern margin off Raukumara Peninsula is characterized by non-accretion and tectonic erosion associated with seamount impact scars (Lewis et al., 1997, 1998, 2004; Collot et al., 2001), whereas the central margin off the Wairarapa coast is a classical imbricated thrust wedge dominated by accretion (Davey et al., 1986b; Lewis and Pettinga, 1993; Collot et al., 1996; Barnes and Mercier de Lépinay, 1997; Lewis et al., 1999). The relatively narrow southern end of the margin lies in the transition from oblique subduction to continental strike-slip deformation (Barnes et al., 1998a; Barnes and Audru, 1999; Holt and Haines, 1995) and is incised by Cook Strait Canyon (Mountjoy et al., 2009).

To a first order, Townend (1997a) estimated that an enormous volume of 24 m^3 of fluid per meter of strike length is added to the Hikurangi Margin by frontal accretion per year. Of that, >80% was inferred to be released by subsequent compaction and tectonic deformation, together with an additional 3 m^3 per meter of strike length per annum released by smectite dehydration at depths of 5–10 km. There is ample evidence of fluid flow within the margin. This includes the many oil, gas and mud expulsion sites observed on land (Field et al., 1997), widespread cold vent seep sites and associated chemosynthetic faunas offshore (Lewis and Marshall, 1996; Faure et al., 2006; Greinert et al., 2010-this issue), the occurrence of direct hydrocarbon indicators in industry seismic reflection data (Frederik, 2004), and a widespread bottom simulating reflection (BSR), interpreted as marking the base of the gas hydrate stability zone (Katz, 1981; Henrys et al., 2003; Pecher et al., 2004, 2005; Henrys et al., in press). Studies of exposed rocks in the forearc basin indicate that fluid seepage has occurred on the margin for at least 22 Myr (Campbell et al., 2008). The BSR has been modelled to reveal low values (44 ± 10 mW m^{-2}) of heat flow (Townend, 1997b; Henrys et al., 2003; Netzeband et al., 2010-this issue). Elevated pore pressures have been commonly encountered in exploration wells (Davies et al., 2000; Darby et al., 2000), and assumed to be widespread within the accretionary wedge (Barnes and Mercier de Lépinay, 1997).

Since 2001, multichannel seismic reflection and high-resolution multibeam bathymetric data have been acquired from the Hikurangi Margin by research institutes, oil companies, and the New Zealand Government as part of hydrocarbon exploration and research initiatives. The improved understanding of tectonic structure that can be gained from these data, combined with the widespread occurrence of gas hydrates and cold seeps makes this margin an excellent example to study the relationship between thrust tectonics and fluid flow. This paper presents a revision and synthesis of the tectonic morphology, fault structure, and composition of the imbricated thrust wedge between Mahia Peninsula and Cook Strait (Fig. 1). We then establish the tectonic and geological framework for each of five study areas with submarine seep sites, and we interpret these sites within the context of regional structural processes. Finally we discuss the role of the deformation structures as fluid conduits.

2. Data used in this study

The continental shelf of the Hikurangi Margin is relatively well covered with multichannel seismic reflection (MCS) data, from which detailed accounts of active tectonics (e.g., Barnes et al., 2002; Barnes and Nicol, 2004; Lewis et al., 2004), sequence stratigraphy (Paquet, 2008; Paquet et al., 2009), and exploration geology (e.g., Field et al., 1997; Uruski et al., 2004) have been published. The continental slope however, is less well surveyed. Previous regional interpretations of the tectonic structure were based largely on *RV L'ATALANTE* SIMRAD EM12Dual multibeam bathymetry and Hawaii MR1 sidescan sonar images, supported by the SP LEE MCS profile, *RV L'ATALANTE* and pre-1980s oil company low-fold MCS data (Fig. 1D), and widespread single channel seismic data (not shown in Fig. 1D) (Davey et al., 1986a,b; Lewis and Pettinga, 1993; Collot et al., 1996; Barnes and Mercier de Lépinay, 1997, Lewis et al., 1997, 1999; Barnes et al., 1998a,b).

MCS data acquired since 2001, and available for this study, includes (Fig. 1D) (1) the GECO RESOLUTION NIGHT high-fold profile off Hawkes Bay (Pecher et al., 2004, 2005; Henrys et al., 2006), (2) the large grid of *MV MULTIWAVE* high-fold MCS data (CM05) from the upper margin off Hawkes Bay and East Coast (Multiwave, 2005; Nicol et al., 2007), (3) low-fold MCS data acquired off Hawkes Bay and Mahia Peninsula on several surveys by *RV TANGAROA* (CR3044, TAN0106, TAN0313, TAN0412) (Barnes et al., 2002; Paquet et al., 2009), and (4) regional low-fold MCS profiles acquired by *RV SONNE* SO191 in 2007 from the central part of the margin.

On the *RV SONNE* SO191 survey in 2007, we acquired a total of 710 km of regional seismic reflection data (red lines in Fig. 1D). An array of five SODERA G-guns with total capacity of 2080 in.^{3} (32 l) was used as the seismic source on lines 1 to 6, and a 250/105 in.^{3} (5.5 l) GI gun on lines 8 to 10. The data were received on a 32 channel digital GEOMETRICS GeoEel hydrophone array. Standard processing included trace editing, correction for spherical divergence energy loss, frequency domain filtering, CDP gather at 12.5 m, Normal Move-Out correction following velocity picking using semblance plots, nominal 4 fold CDP stack, and finite difference time migration. In addition to the regional seismic lines, we acquired about 415 km of high-resolution MCS data from the Wairarapa, Uruti Ridge, Omakere Ridge and Builders Pencil seep sites (Fig. 1B) using a 250/105 in.^{3} GI gun source and SIG 4-channel towed streamer (e.g., Netzeband et al., 2010-this issue).

Greinert et al. (2010-this issue) outlined new multibeam bathymetry data available to this study, including 30 kHz SIMRAD EM300 data acquired on *RV TANGAROA* surveys TAN0616 and TAN0607, and 12 kHz SIMRAD EM120 data acquired on *RV SONNE* SO191. In addition to these data, and archived SIMRAD EM12Dual L'ATALANTE data, we have also used SIMRAD EM300 multibeam data collected over the southern Wairarapa region on *RV TANGAROA* surveys TAN0215, TAN0309, and TAN0510 (Mountjoy et al., 2009), and over the Poverty Seavalleys off Mahia Peninsula on TAN0106. These data have been processed to variable grids of 10 m to 30 m resolution. The Hawaii MR1 sidescan sonar data previously presented by Barnes and Mercier de Lépinay (1997) and Lewis et al. (1998) have been reinterpreted in light of the new multibeam bathymetric and seismic reflection data. In discussion of bathymetric features, we refer to Mitchell (1988), Arron and Lewis (1992), and Garlick and Mitchell (2002).

3. Tectonic and stratigraphic architecture of the Hikurangi Margin

3.1. Composition of the imbricated frontal wedge

The Hikurangi Margin comprises a thrust imbricated frontal wedge up to 150 km in width (Lewis and Pettinga, 1993). It is built against a Mesozoic basement backstop of Torlesse terrane greywackes. These latter rocks developed on the active margin of Gondwana supercontinent, and are now exposed in the axial ranges of North Island, Raukumara Peninsula, and the coastal hills of southern Wairarapa (Fig. 1). The imbricated frontal wedge extends eastwards across the coastal ranges and offshore margin, where it has a ridge and basin morphology (Fig. 2). The wedge comprises three major components, all of which are deforming together as one sedimentary body. These include (1) an inner foundation of Late Cretaceous and Paleogene, pre-subduction rocks (Figs. 3 and 4); (2) an outer wedge of late Cenozoic accreted trench-fill turbidites; and (3) a deforming cover sequence of Miocene to Recent shelf and slope basin sediments, which are up to several kilometers thick beneath the upper margin and generally thin seawards over the frontal accretionary wedge. The deforming cover sequences of the upper margin are partially exposed in uplifted forearc basins on land, and at structural ridges offshore, and exhibit sequence architectures that are strongly influenced by sea-level cycles and active tectonics (e.g., Lewis, 1973; Barnes et al., 2002; Paquet, 2008; Paquet et al., 2009). The cover sequences include terrestrial, nearshore marine, shelf, and slope sediments.

The inner, Late Cretaceous and Paleogene foundation was deposited prior to initiation of Hikurangi subduction, and subsequently became highly imbricated as a result of poly-phase deformation following the onset of subduction some 25 Myr ago (Ballance, 1976; Rait et al., 1991; Lewis and Pettinga, 1993; Field et al., 1997; Barnes et al., 2002; Barnes and Nicol, 2004, Henrys et al., 2006; Nicol et al., 2007). Whilst substantial deformation of these rocks occurred in the Miocene, active thrust faulting and folding continues across the inner margin to present day. These rocks produce highly disrupted seismic reflections, with footwall and hanging wall cutoffs typical of thrust tectonic geometries (e.g., Figs. 3 and 4). The rocks outcrop widely along the coast where they exhibit complex mesoscopic deformation fabrics (Pettinga, 1982), have been encountered in a drill hole in Hawke Bay, and dredged from structural highs both within and offshore of Hawke Bay (Lewis and Pettinga, 1993; Lewis and Marshall, 1996; Barnes et al., 2002). In the middle slope region these rocks are typically characterized by variable amplitude, relatively discontinuous, and complex seismic reflections, compared to the accreted turbidites beneath the lower slope (Figs. 5 and 6).

The outer wedge of accreted late Cenozoic turbidites is thrust beneath the front of the inner foundation (Figs. 3–5). This frontal wedge is highly imbricated and produces characteristic seismic reflections correlated with the Hikurangi Trough sequence, which is described in Section 3.3. We have identified the contact between these two components of the imbricated frontal wedge to within c. 10 km in widely spaced (~35 km) seismic profiles along the margin, and have revised its position in Figs. 1 and 2A relative to previous interpretations (Lewis and Pettinga, 1993; Lewis et al., 1997, 1999; Barnes and Mercier de Lépinay, 1997; Barnes et al., 1998a,b).

3.2. Lateral variations in structural and morphological development of the margin

The overall morphology of the Hikurangi Margin varies significantly along strike as a result of variations in the thickness of trench-fill sediment, efficiency of frontal accretion, smoothness/roughness of the Pacific Plate, and obliquity and rate of convergence (Lewis and Pettinga, 1993). Because the trough and its axial channel are supplied with turbiditic sediment largely from submarine canyons in the south (Lewis et al., 1998; Lewis and Barnes, 1999; Mountjoy et al., 2009), the thickness of the turbidites decreases northwards from more than 5 km near Cook Strait to about 1 km off the Raukumara Peninsula (Fig. 1B). Whereas trench-fill sediment thickness decreases northwards, the rate of convergence between the forearc and the subducting Pacific Plate increases northwards by three times, from about 20 mm/yr off southern Wairarapa to nearly 60 mm/yr off the Raukumara Peninsula (Wallace et al., 2004) (Fig. 1B). These variations coincide with relatively low relief on the southern part of the subducting Hikurangi Plateau, compared to the seamount studded northern region, where basement relief commonly exceeds several kilometers (e.g., Figs. 1 and 4) (Wood and Davy, 1994; Davy and Wood, 1994; Lewis et al., 1998; Davy et al., 2008).

Along the northern half of the margin, the combination of relatively thin trench-fill sediment (~1 km), high convergence rate, and rough topography of the subducting plate promotes non-accretion, localized tectonic erosion, and deformation processes within the frontal wedge that reflect the progressive passage of basement asperities beneath the margin (Collot et al., 1996, 2001; Lewis et al., 1997, 1998, 2004; Pecher et al., 2005). The lower margin between the bathymetric bank referred to informally as Rock Garden and the southern Kermadec Trench, is typically about 50–60 km in width, has a relatively steep gradient (>10°), and is characterized by large seamount impact scars, particularly at Poverty Seavalleys and East Cape (Figs. 1 and 2B).

The NIGHT seismic reflection profile off Hawke Bay (Fig. 4) is reasonably representative of the northern half of the margin. It shows a clear interplate thrust décollement extending to 6–8 s TWT (ca. 12–15 km) beneath the coastal region, numerous upper plate thrusts, and a seamount subducted beneath the outer margin bank referred to informally as Rock Garden (Fig. 2) (Pecher et al., 2004, 2005; Henrys et al., 2006). The upper margin structures are correlated to and mapped with an extensive set of high-quality industry and research seismic sections, and they include reactivated thrusts, inversion structures, and thrust triangle zones (Barnes et al., 2002; Barnes and

Fig. 1. A. Overview of the Pacific–Australia plate boundary in the New Zealand region, showing the Kermadec–Hikurangi subduction zone. B. Morphology and major active faults of the Hikurangi Subduction margin. Bold thrust is the principal deformation front. Isopachs in the Hikurangi Trough indicate approximate thickness (km) of trench-fill turbidites (Lewis et al., 1998). Bold black numbers along the deformation front are modelled convergence rates (mm/yr) between the Hikurangi Margin and the Pacific Plate (Wallace et al., 2004). Plate motion vectors are from Beavan et al. (2002). The bold dashed white line along the middle slope separates the late Cenozoic frontal accretionary wedge beneath lower continental slope from a deforming foundation of pre-subduction, Cretaceous and Paleogene passive margin rocks and overlying Miocene to Recent slope basins beneath the middle to upper margin. The bold black line in the Hikurangi Trough is the meandering Hikurangi Channel. Labels Wairarapa, Uruti Ridge, Porangahau Ridge, Omakere Ridge, Rock Garden, and Builders Pencil are seep sites discussed in this paper and elsewhere in this issue. LR, Lachlan Ridge; RR, Ritchie Ridge. C. Schematic section across the Hikurangi subduction zone, axial ranges of North Island, and back arc volcanic rift. Shading with wavy line pattern is Mesozoic Torlesse basement rocks. Smooth grey shade is deforming Cretaceous and Paleogene pre-subduction sequences with Miocene to Recent slope basins, and white is accreted trench-fill turbidites. D. Distribution of regional multichannel seismic reflection coverage across the Hikurangi Margin. Notable surveys include GECO RESOLUTION 2001 NIGHT high-fold profile, grey line off Hawkes Bay; *RV TANGAROA* low-fold data, purple lines off Hawkes Bay and Mahia; *MV MULTIWAVE* 2005 high-fold CM05 profiles, black lines (profile labeled 1 is CM05#1); *RV SONNE* SO191 2007 regional low-fold profiles, red lines; *RV SP LEE* 1983 high-fold profile, dark blue line across central margin; *RV L'ATALANTE* 1993 "GeodyNZ" low-fold profiles, gold lines. (For interpretation of the references to colour in this figure legend, the reader is referred to the web version of this article.)

Nicol, 2004). Depth conversion using wide-angle velocity control indicates that the subducted seamount beneath the lower margin has about 3 km of basement relief (Fig. 4 inset). The plate boundary décollement and the overriding ridge above the seamount have been uplifted (Fig. 7), and upper plate thrust faulting is now focused beneath the northern Paoanui Ridge, along the landward side of the elevation (Fig. 2A). Inactive thrusts imaged beneath the steep seaward flank of the ridge have been abandoned in the wake of the seamount,

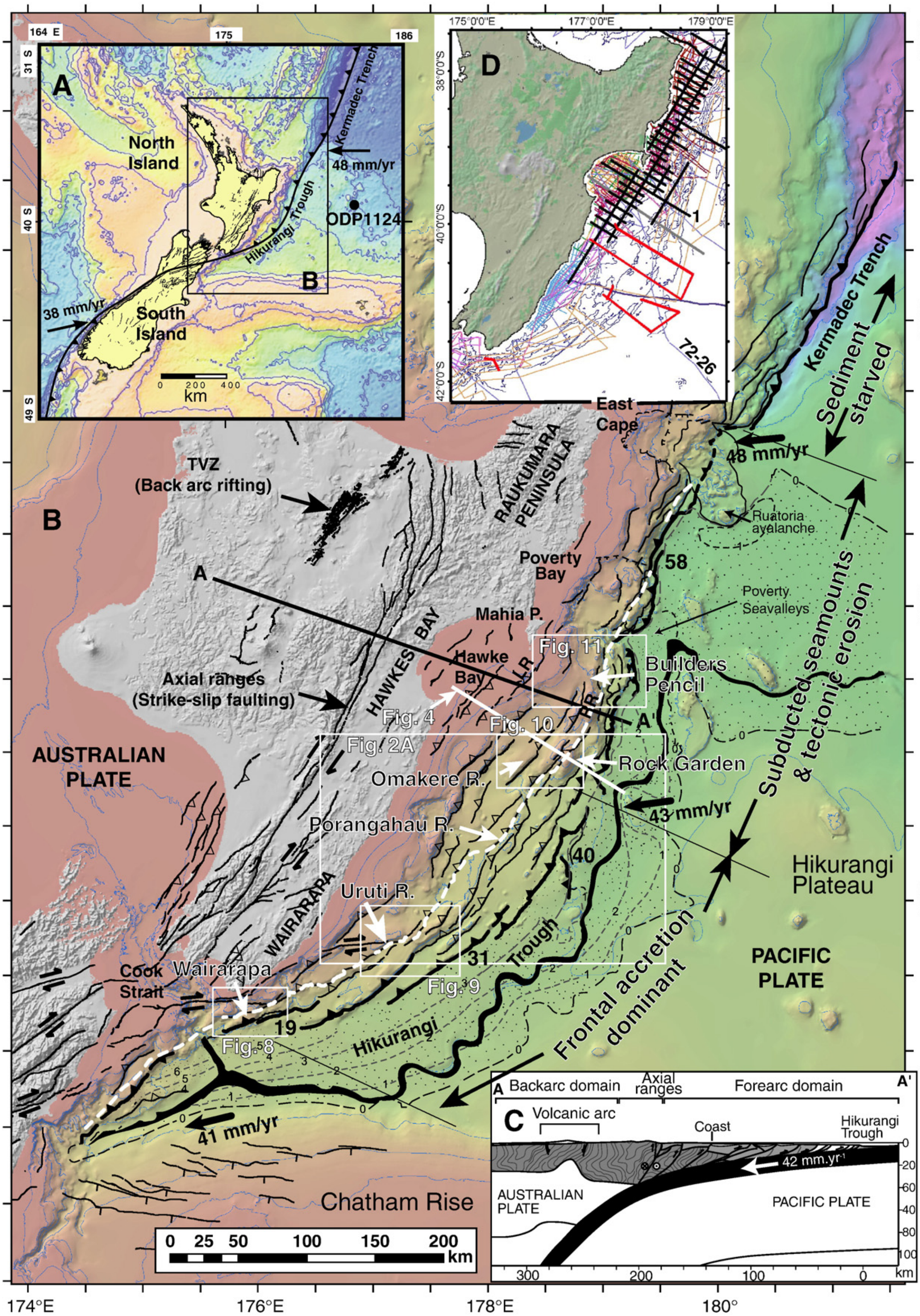

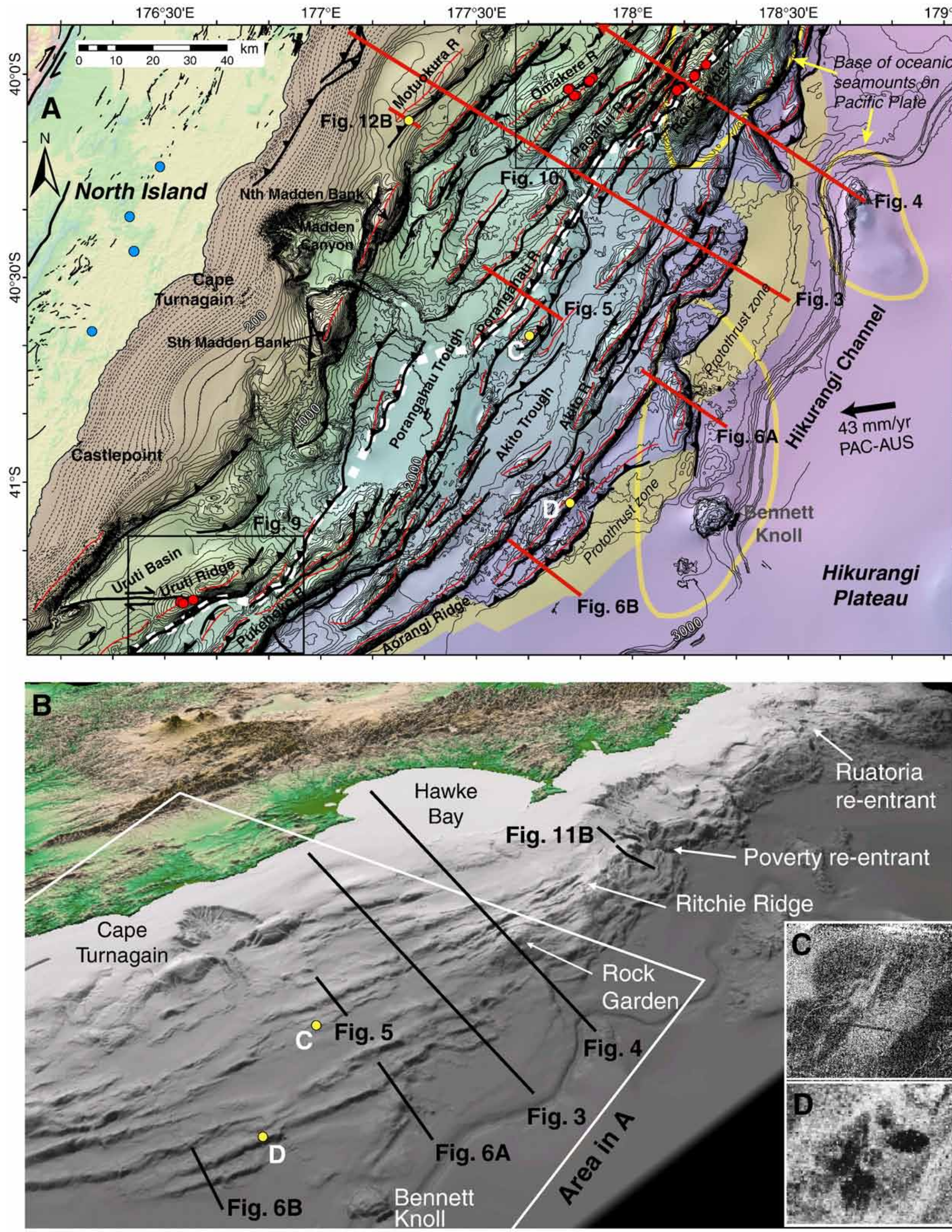

Fig. 2. A. Bathymetry and major tectonic structures of the central section of the Hikurangi Margin, interpreted as part of this study, and modified significantly from Lewis et al. (1999). Red lines are crests of thrust-faulted bathymetric ridges, and represent a close proxy to the axial traces of anticlines imaged in seismic sections. Bathymetric labels are in metres. The protothrust zone is shaded mustard yellow. Onshore active faults are courtesy of the GNS Science active faults database. The bold dashed white line along the middle slope separates the late Cenozoic frontal accretionary wedge beneath lower continental slope from a deforming foundation of pre-subduction, Cretaceous and Paleogene passive margin rocks and overlying Miocene to Recent slope basins beneath the middle to upper margin. Plate motion vector is from Beavan et al. (2002). Bold yellow ellipses are the bases of oceanic seamounts on the subducting Pacific Plate. Note the northern of these underlies Rock Garden, whereas the southern partially underlies the present deformation front. Blue bold dots are active seep sites on land. Red dots are seep sites discussed in this issue. Yellow dots are other sites of suspected fluid expulsion from seismic reflection and MR1 deep-tow sidescan sonar data. B. Oblique view of hillshaded bathymetry derived from 100 m grid data. C. MR1 sidescan image of suspected fluid expulsion site surrounded by possible radiating mud flows. D. MR1 sidescan image of suspected mud volcano (Barnes and Mercier de Lépinay, 1997).

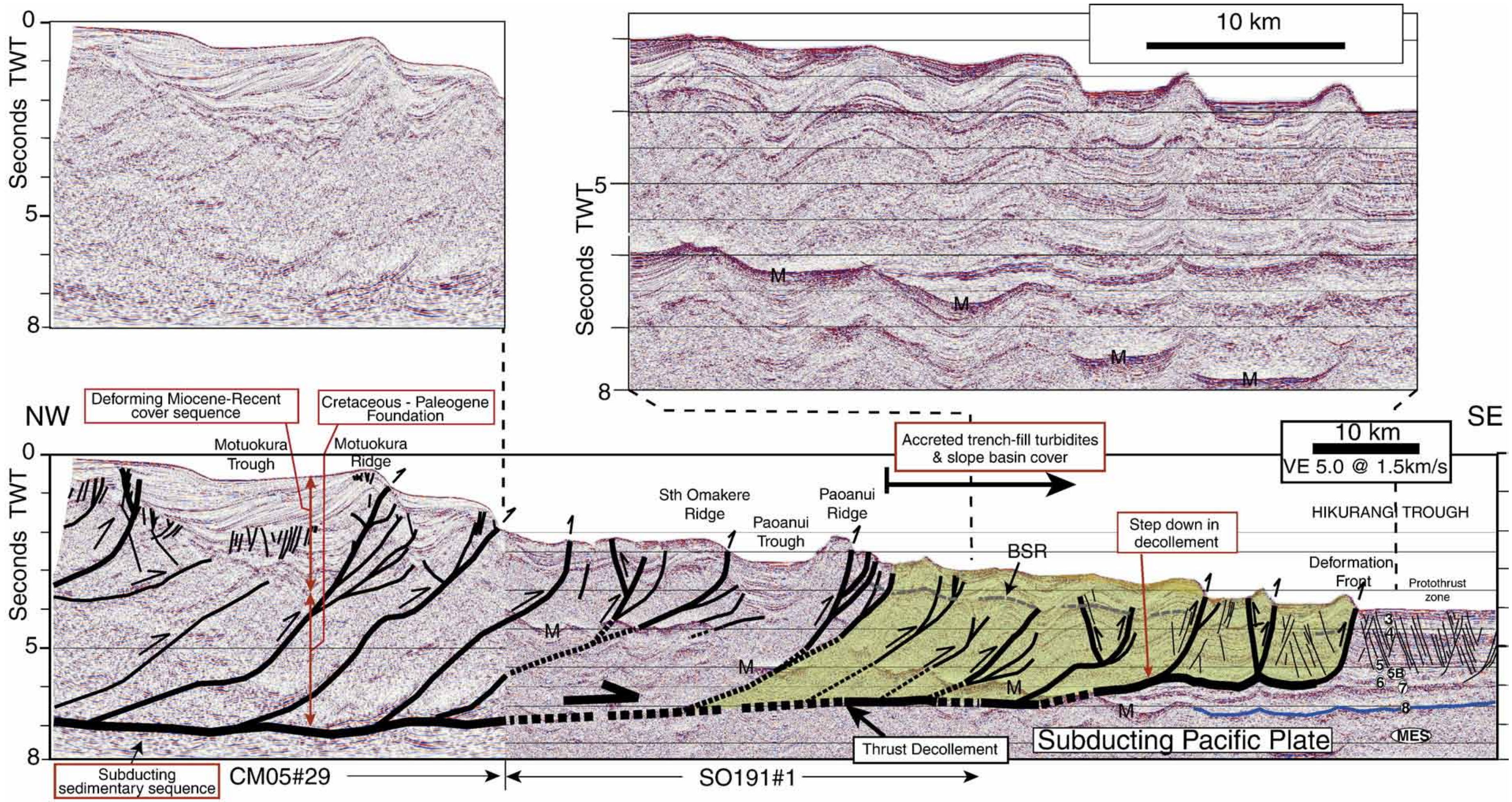

Fig. 3. Uninterpreted and interpreted multichannel seismic section across the central Hikurangi Margin. The seismic data are two spliced sections, including high-fold seismic data across the continental shelf (CM05#29) and low-fold data across the slope and trough (SO191#1). Profile locations are shown in Fig. 2. Note that structures illustrated are reproductions of interpretations originally made in detail on large sections with low (2.5×) vertical exaggeration. This transect is representative of the more classical accretionary structure and processes dominating the margin south of Rock Garden. M is the first seafloor multiple. Numbered reflections in the trench sequence are from Barnes and Mercier de Lépinay (1997) and this study (see Fig. 6B). The dotted lines in the lower centre of the low-fold profile are hypothetical extensions of the faults beneath the multiple.

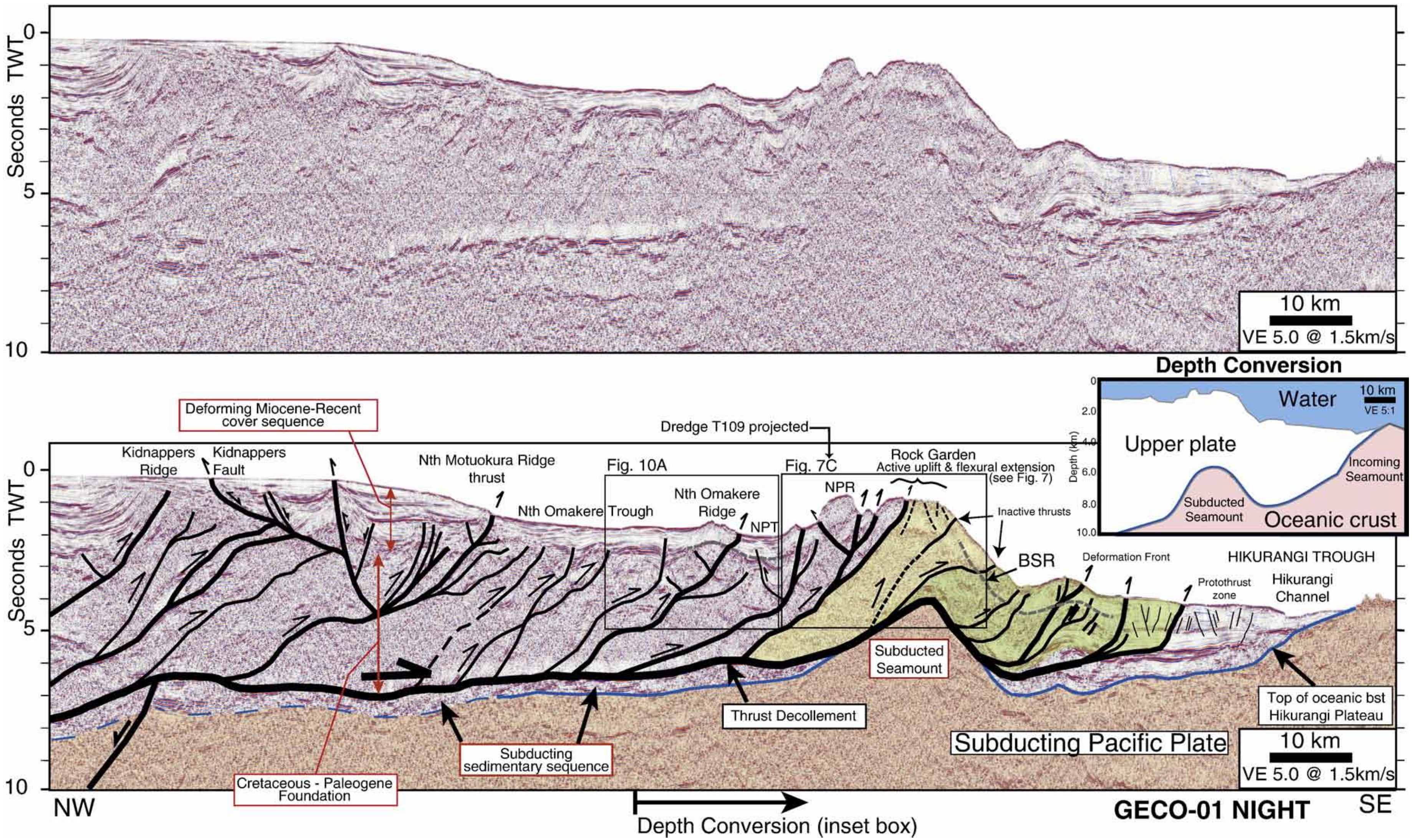

Fig. 4. Uninterpreted and interpreted high-fold NIGHT multichannel seismic section acquired by GNS Science on *MV GECO RESOLUTION* across the Hawke Bay margin, Rock Garden, and a subducting seamount. This section is representative of the structure and processes dominating the northern Hikurangi Margin between Rock Garden and East Cape. Upper margin structures are correlated to and mapped with an extensive set of high-quality industry and research seismic sections (Barnes et al., 2002; Barnes and Nicol, 2004). Bold faults are considered to be active. NPT, northern Paoanui Trough; NPR, northern Paoanui Ridge. The green shading is the extent of the accreted trench-fill section (yellow shading indicates region of compositional uncertainty at the rear of the wedge). The inset shows the plate interface in the frontal half of the section depth converted using velocities derived from wide-angle reflection data.

whereas active frontal thrust faulting has since re-established in the Hikurangi Trough sequence to the east. A similar tectonic history is recorded on profile CM05#1 across Ritchie Ridge 30 km to the north (Fig. 1B and D) (e.g., see Fig. 8 of Nicol et al., 2007).

As a result of seamount subduction beneath the Rock Garden, numerous cross-cutting faults are developed on the seafloor over the crest of the bank (Fig. 7A and B) (Pecher et al., 2005; Faure et al., 2006). These structures produce bathymetric scarps typically a few tens of meters in height on the eroded crest of the bank, and they exhibit a landward diverging radial pattern. They appear to be superimposed over a major NE–SW striking thrust scarp, which may or may not be currently active. The observed fault array is analogous to those produced in laboratory sandbox experiments of deformation above subducting asperities (e.g., Dominguez et al., 1998; Lewis et al., 2004) and observed elsewhere in other natural examples (e.g., Huhnerbach et al., 2005). Major collapse of the margin in the wake of the seamount, at the scale evidenced further north at Poverty Seavalleys and at Ruatoria Avalanche (e.g., Lewis et al., 1998; Collot et al., 2001), has not occurred yet indicating that it is a later deformation stage that will occur when the seamount passes further landward (e.g., Von Huene and Lallemand, 1990) or perhaps that some seamounts previously subducted further north had different geometry and/or substantially greater relief.

Compared to the northern margin, the tectonic accretion that dominates the central margin off southern Hawkes Bay and Wairarapa has been facilitated by thicker trench-fill sediment (~3–4 km), relatively smooth and sediment-covered subducting plate, and slower (by ~20 mm/yr) rate of convergence (Fig. 1) (Davey et al., 1986a; Lewis and Pettinga, 1993; Barnes and Mercier de Lépinay, 1997; Lewis et al., 1999; Wallace et al., 2004). East of Cape Turnagain, where the deformation front lies up to 130 km offshore, the frontal accretionary wedge reaches 65–70 km in width (Figs. 2 and 3). The transition between the inner foundation of imbricated passive margin rocks and accreted trench-fill turbidites (e.g., Fig. 5) is interpreted to lie seaward of Uruti, Porangahau and Paoanui ridges (Fig. 2A). Although a series of apparent right steps in this transition potentially mirrors the shape of the deformation front, the overall structure and morphology of the wedge indicates that its growth has not been significantly perturbed by relief on the subducting plate for at least 1–2 Myr. The exception to this is where the northern end of Bennett Knoll seamount ridge, which is about 80 km in length and has relief of several kilometers, is presently subducting beneath the deformation front east of Akito Ridge (Figs. 2 and 6A).

The repetitive ridge and basin morphology across the central margin reflects up to 10 major seaward-vergent thrust faults between the shelf and Hikurangi Trough. The longer thrust systems reach up to 120 km in length (Figs. 1 and 2). On the whole, the crests of successive ridges become progressively deeper seaward. Individual ridges typically have up to about 1 km of bathymetric relief, and an asymmetric profile, with a relatively gentle landward (back) limb and steeper seaward (fore) limb. Thrust faults generally steepen upward in the sedimentary section from dips of <20° in the lower part of the wedge to as much as 40–50° in the upper 1 km or so near the deformation front. Barnes and Mercier de Lépinay (1997) identified the fault growth sequence on the back limbs of the thrust ridges within the frontal 30 km of the wedge (e.g., Fig. 6) and estimated the horizontal shortening of the turbidite sequence there to be of the order of 6 km. They interpreted that 80% of this shortening occurred within 0.4 ± 0.1 Myr, at an average rate of 12 ± 3 mm/yr. They also inferred that the deformation front had advanced seaward by as much as 50 km since about 0.5 Ma, an observation consistent with the recent results of Nicol et al. (2007).

3.3. The Hikurangi Trough and the subducting Hikurangi Plateau sequence

The Hikurangi Trough sedimentary sequence and the top of the subducting Hikurangi Plateau is imaged well in our new seismic sections (Figs. 3 and 6B). We correlated the seismic stratigraphy in the trough, imaged on the *RV SONNE* profiles at about 41°S (Fig. 6B), with

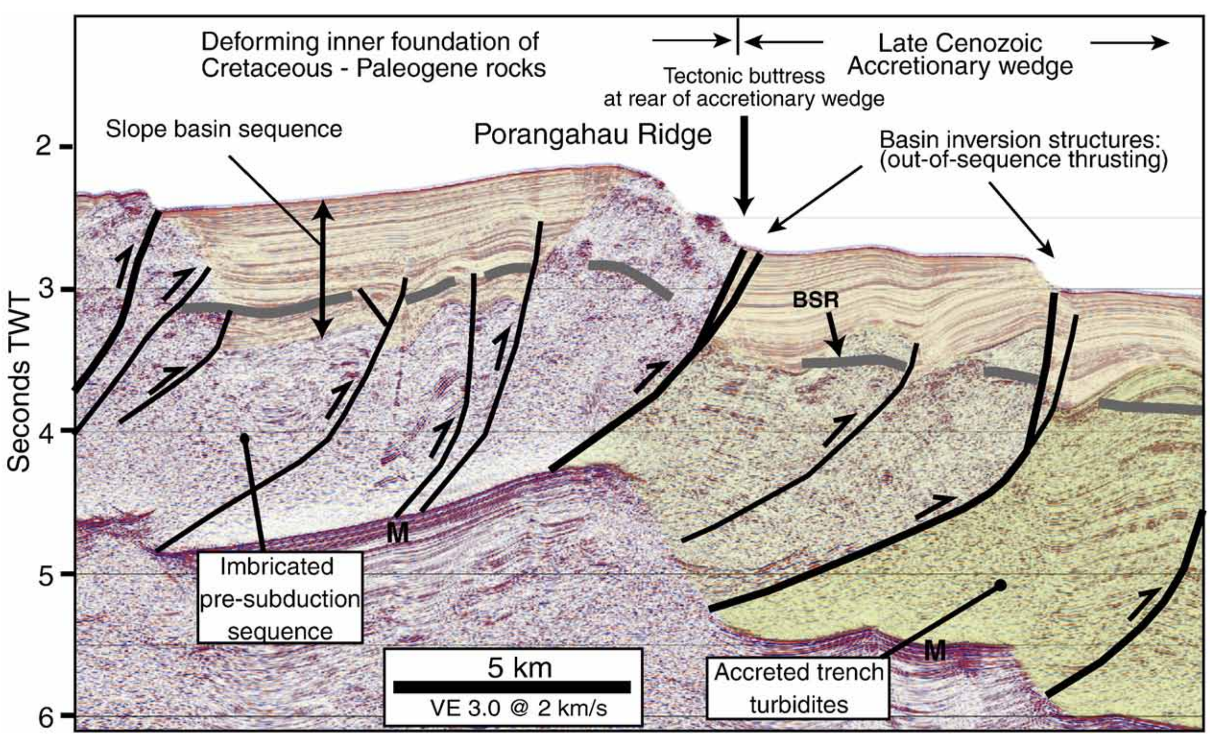

Fig. 5. Part of multichannel seismic section SO191#3 illustrating the contact between the outer edge of the imbricated Cretaceous–Paleogene foundation rocks and the landward part of the late Cenozoic accretionary wedge (bold dashed white line in Figs. 1 and 2A). All seep sites documented in this study lie above or relatively near this contact. The contact is imaged as a boundary marking a significant change in seismic reflectivity, somewhat transitional where indicated by the intermediate shading. The reflectivity changes from relatively coherent accreted trench-fill turbidite reflections to an acoustically chaotic foundation of complexly deformed pre-subduction stratigraphy landward. These units are variably covered by deforming slope basins, and there is a discontinuous BSR. Profile location is shown in Fig. 2.

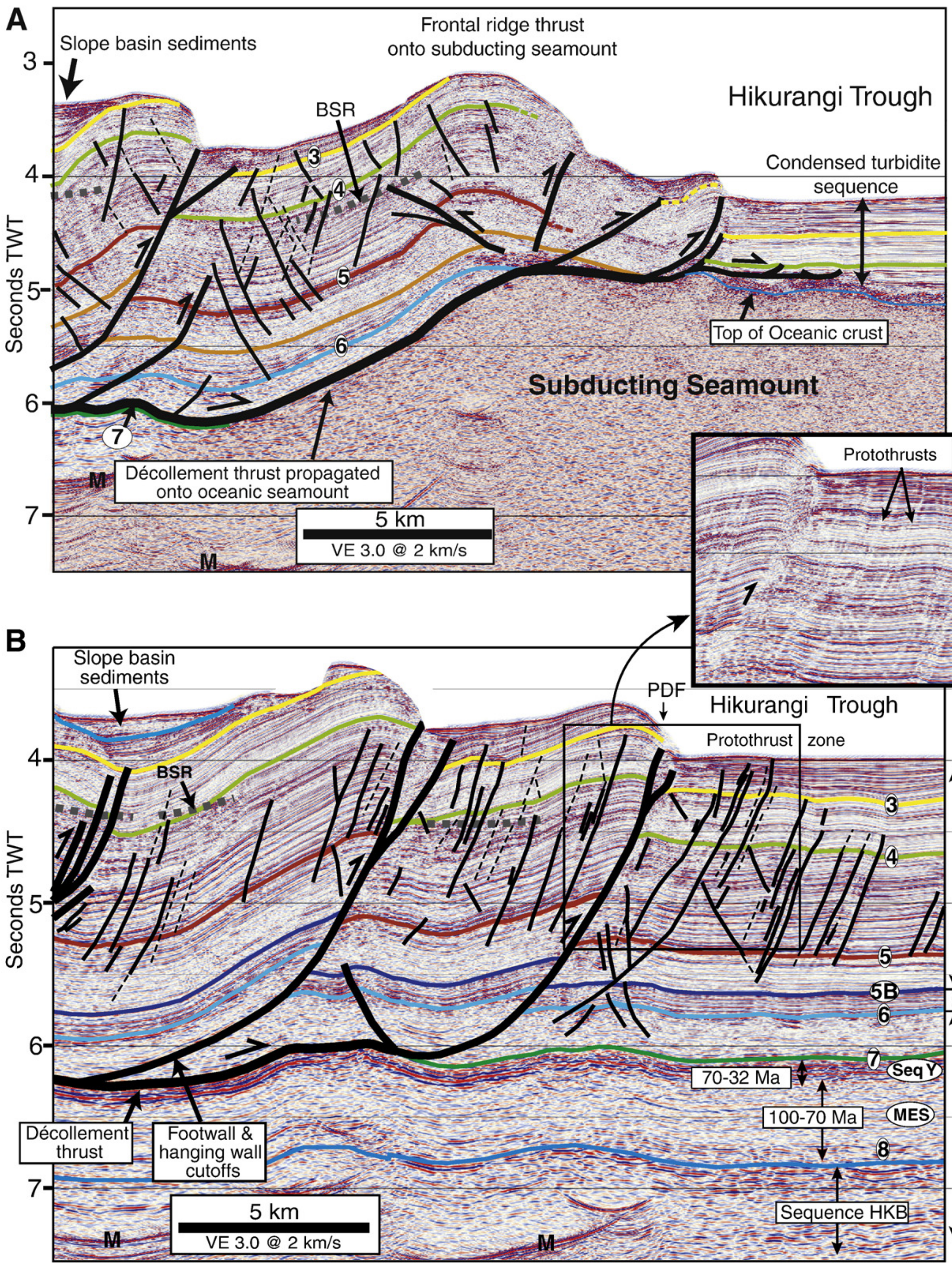

Fig. 6. Multichannel seismic sections illustrating examples of active tectonic structures across the central Hikurangi Margin deformation front. A. Part of SO191#3 showing incipient subduction of the Bennett Knoll seamount complex, causing increased uplift of the frontal ridge. B. Part of SO191#6 across classic frontal accretionary thrusts. The inset illustrates protothrusts. PDF, principal deformation front. Trench-fill stratigraphy in both sections, included numbered reflections, is from Barnes and Mercier de Lépinay (1997) and this study. Profile locations are shown in Fig. 2.

archived *RV L'ATALANTE* profiles (Barnes and Mercier de Lépinay, 1997) and with Mobil oil company profile 72–26 (Fig. 1D). The later profile extends southeast of the axial turbidite system and onto the Hikurangi Plateau north of the Chatham Rise, where a widespread seismic stratigraphy has been established by Davy et al. (2008). Davy et al. (2008) considered seismic velocities, tied reflections to ODP 1124 (Fig. 1A) and to rock dredge samples, and compared sections with dated sequences on the Manihiki Plateau, which is thought to have rifted from the Hikurangi Plateau in the Cretaceous. Although line 72–26 cannot be tied directly to profiles located further east presented by

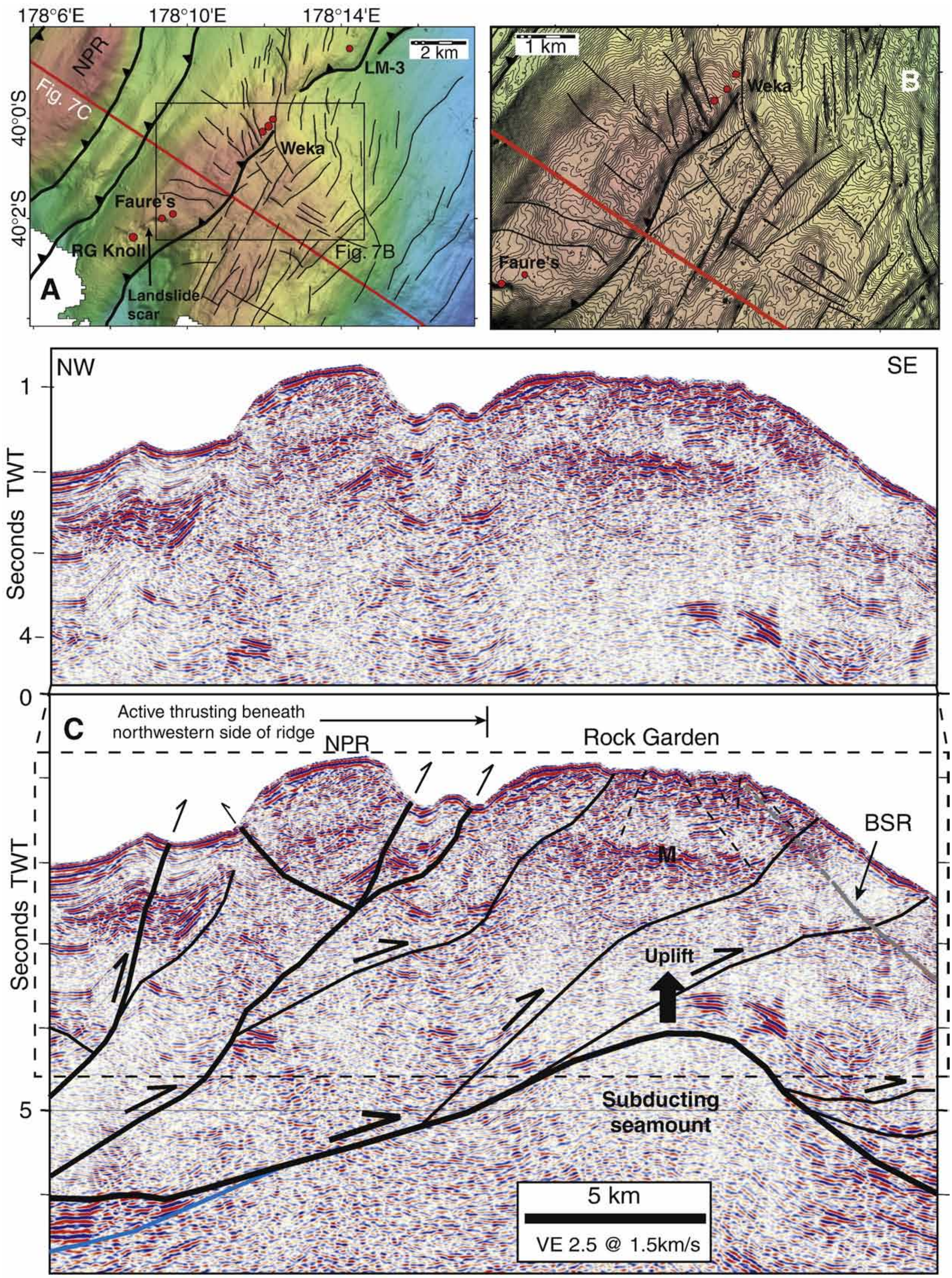

Fig. 7. A. Bathymetric and structural map of Rock Garden developed from 25 m binned, *RV TANGAROA* SIMRAD EM300 multibeam data. Location of A is shown in Fig. 10. B. Detail of bathymetric contours at 5 m interval. Location of B is shown in A. NPR, northern Paoanui Ridge. Red dots are seep sites. C. Uninterpreted and interpreted part of high-fold NIGHT multichannel seismic section, revealing active thrusts beneath the western side of the ridge and a subducting seamount driving uplift and extension of the Rock Garden. M is the first seafloor multiple.

Davy et al. (2008) (e.g., profile HKDC1), we recognize the same seismic stratigraphy of the plateau sequence in line 72–26, based on very similar reflection characteristics and two way travel time (TWT) depths. Our correlations between the Hikurangi Trough and the Hikurangi Plateau sequences identified by Davy et al. (2008) provide the first insights into the nature of the sedimentary sequence within which the interplate thrust is developed (see Section 3.4).

Our correlations indicate that in the central Hikurangi Trough reflection 8 (Fig. 6B) is approximately equivalent to the top of unit HKB of Davy et al. (2008). This unit has been interpreted as Early Cretaceous (>100 Ma) volcaniclastic sediments and/or limestone/chert with relatively low seismic velocities (~2.4–3.5 km/s) compared to the underlying basaltic basement rocks (>4 km/s) (not imaged in Fig. 6B). Reflection 8 is overlain by a c. 0.5 s TWT thick sequence (~575–650 m, assuming 2.3–2.6 km/s interval velocities) of weaker reflectivity. This sequence correlates with unit MES of Davy et al. (2008), inferred to represent Cretaceous (100–70 Ma) clastic sedimentary rocks. These rocks are overlain by a uniformly thick (0.15 s TWT, c. 170–250 m) sequence of widely traceable, high-amplitude reflections beneath reflector 7. This interval is the Hikurangi Plateau sequence Y of Wood and Davy (1994), identified by Davy et al. (2008) as Late Cretaceous–Early Oligocene (70–32 Ma) nannofossil chalks with alternating mudstones. Above this interval, the upper part of the Hikurangi Plateau sequence, which reaches 1.4 s TWT thickness east of the Hikurangi Trough, includes the 0.3 s TWT thick, weakly reflective interval between reflectors 6 and 7 (Fig. 6B). This interval is inferred to correlate with nannofossil chalks interbedded with tephras and clays at ODP 1124 (Fig. 1A). The upper plateau sequence may also include the interval of high-amplitude reflections between reflectors 5B and 6. Reflector 5B is locally a strong erosion surface, above which are easterly onlapping, coherent reflections from trench turbidites (Figs. 3 and 6) associated with local paleo-channels and channel levee sediment waves (see also Lewis et al., 1998). Although not directly dated, reflectors 3, 4 and 5 (Fig. 6) were inferred by Barnes and Mercier de Lépinay (1997) to be of the order of 0.8 Ma, 2.0 Ma, and 5.0 Ma, respectively.

3.4. Décollement position and protothrust zone

The refined seismic stratigraphy of the Hikurangi Trough sequence and clear imaging of the frontal deformation structures in the *RV SONNE* SO191 profiles enables improved identification of the interplate thrust where it is propagating into the trench sediments (Fig. 6B). The interplate thrust is recognized as the major décollement, above which the accreted sequence is shortening by distributed thrust faulting and folding, and below which undeformed sediments are being subducted. Near the front of the wedge, the stratigraphic position of the décollement is tightly constrained to within a couple of wavelets of the seismic data, by recognition of the down-dip extent of the accretionary thrusts from observations of inclined hanging wall reflections, and foot wall reflection cutoffs (e.g., Fig. 6B).

In the centre of the margin west of Bennett Knoll the décollement coincides with reflector 7 for at least 30 km down dip (Fig. 6B). This position, within the pelagic sediments (nannofossil chalks, tephras, mudstone, clays) of the Hikurangi Plateau sequence, is some 400–450 m stratigraphically below what are clearly turbidites. Immediately below the décollement are unfaulted high-amplitude reflections correlated with Late Cretaceous–Early Oligocene (70–32 Ma) nannofossil chalks and alternating mudstones. Immediately above it is the thrusted sequence inferred to be Cenozoic (probably Miocene) alternating chalk, tephras and clays. In comparison, on profile SO191#1 (Fig. 3), about 100 km to the northeast, the frontal 15 km of the décollement is developed at a stratigraphic position about 0.3–0.4 s TWT (~300–400 m) higher in the plateau sequence. There, it lies just below reflection 5B before stepping down to reflector 7 beneath the third major thrust landward of the deformation front and continuing at that stratigraphic position landwards for at least 15 km down dip. Off the southern Wairarapa coast about 150 km to the southwest of Bennett Knoll, the décollement imaged in archived seismic data is less well constrained, but appears to be developing at the deformation front at a stratigraphic position close to reflector 6 (Barnes and Mercier de Lépinay, 1997). Thus, we recognize in the *RV SONNE* seismic sections that the décollement coincides primarily with reflection 7 in the Hikurangi Plateau pelagic sequence, but that over lateral distances of 100–150 km, its stratigraphic position varies by up to 300–400 m within up to 15 km of the deformation front.

The new seismic profiles combined with archived data also provide new insights into the distribution of a conspicuous protothrust zone in the Hikurangi Trough (Figs. 3 and 6B). Protothrusts were previously recognized mainly west of Bennett Knoll seamount, where they have been interpreted as fluid conduits in an incipient zone of compression between the incoming seamount and the deformation front (e.g., Davey et al., 1986a,b; Lewis and Pettinga, 1993; Barnes and Mercier de Lépinay, 1997; Lewis et al., 1998). It is now clear that the protothrust zone is developed in the turbidite sequence of the Pacific Plate for over 200 km along the central margin (Fig. 2A), and formed not in response to local seamount collision, but primarily to deformation and dewatering associated with forward propagation of the décollement into the trench sequence. The zone is developed up to 20 km seaward of the frontal ridge, in the stratigraphic sequence above the reflector at which the primary thrust décollement is developed further landward (Figs. 3 and 6B). Protothrusts are also clearly imaged in the hanging wall sequence of the frontal two or three major structures in the accretionary wedge, and appear to have been transferred to the wedge (i.e., captured by the Australian Plate) as the décollement and principal deformation front have propagated seawards. The protothrusts are characterized by weak reflectivity (Fig. 6B inset), and dips of the order of $40 \pm 5°$, which is similar to the dip typical of the shallow part of the frontal thrust. The protothrusts imaged in the seismic data have fault spacing typically of several hundred meters to 1 km, with displacements typically of up to a few tens of meters. Although conjugate faults are present (Fig. 6B inset), the dominant vergence is seaward (i.e., northwest dipping faults) west and south of Bennett Knoll, and landward (south east dipping) north of Bennett Knoll (Fig. 3). Similar structures in the Nankai Trough (e.g., Moore et al., 1990) have been interpreted as evolving arrays of brittle–ductile shears that undergo rotation as a result of larger scale ductile flow (Karig and Lundberg, 1990).

4. Tectonic and stratigraphic framework of known seep sites

Elsewhere in this issue, other papers present detailed studies of gas hydrates, geophysically imaged gas plumbing systems, heat flow, fluid seepage, seabed substrate and biological fauna at sites referred to as Wairarapa, Uruti Ridge, Porangahau Ridge, Omakere Ridge, Rock Garden, and Builders Pencil (Fig. 1) (Greinert et al., 2010-this issue; and other papers herein). In the following sections of this paper we outline the distribution of these sites with respect to the major fault structures, tectonic morphology, and stratigraphy.

4.1. Wairarapa sites

The Wairarapa sites lie in the narrowest part of the Hikurangi Margin, some 15–25 km south east of Cape Palliser (Fig. 8). Three major subparallel fault systems dominate the tectonic structure of this part of the margin. From north to south, these include the strike-slip Boo Boo Fault, which extends from the north eastern shelf of South Island into the upper slope area 4–10 km north of the seep sites, and the Opouawe–Uruti and Pahaua thrust faults which underlie the mid-slope bathymetric banks on which the seeps are developed (Barnes and Mercier de Lépinay, 1997; Barnes et al., 1998a; Mountjoy et al., 2009). The region is incised by submarine canyons including Opouawe and Palliser canyons, and is heavily scarred by active submarine landslide systems.

Five seep sites, namely Takahe, North Tower, South Tower, Pukeko and Ruru, lie on Opouawe Bank, typically in about 1000–1100 m water depth. Seismic data show that these sites have developed on the hanging wall of the Pahaua Fault (Fig. 8B), which is characterized by several imbricates that break out as segmented traces on the steep southern forelimb of the bank. These imbricate traces are clearly expressed in the high-resolution EM300 multibeam data, as obvious inflections in the slope gradient, cutting across ridge and gully systems. The other three sites, including Tuatara and Tui on the upper Opouawe Bank, and Miromiro on the western edge of Palliser Bank, lie on the hanging wall sequence of the Opouawe–Uruti Fault in about 850–900 m water depth. This fault similarly breaks out on the seabed as several discontinuous traces on the gullied forelimb of Palliser and Pahaua banks, but its tip is covered by landslide debris in Opouawe Canyon (Fig. 8B), and is blind at about 0.5 s TWT depth beneath the upper Opouawe Bank on seismic profile P036 (see Fig. 4 of Netzeband et al., 2010-this issue).

Regional seismic reflection profiles show that the sedimentary sequence seaward of the Pahaua Fault is trench turbidites (Barnes and Mercier de Lépinay, 1997; Barnes et al., 1998a; Lewis et al., 1998). Although the available seismic data illustrated in Fig. 8B are not of the same quality as in Figs. 3–7, we infer that the Cretaceous and

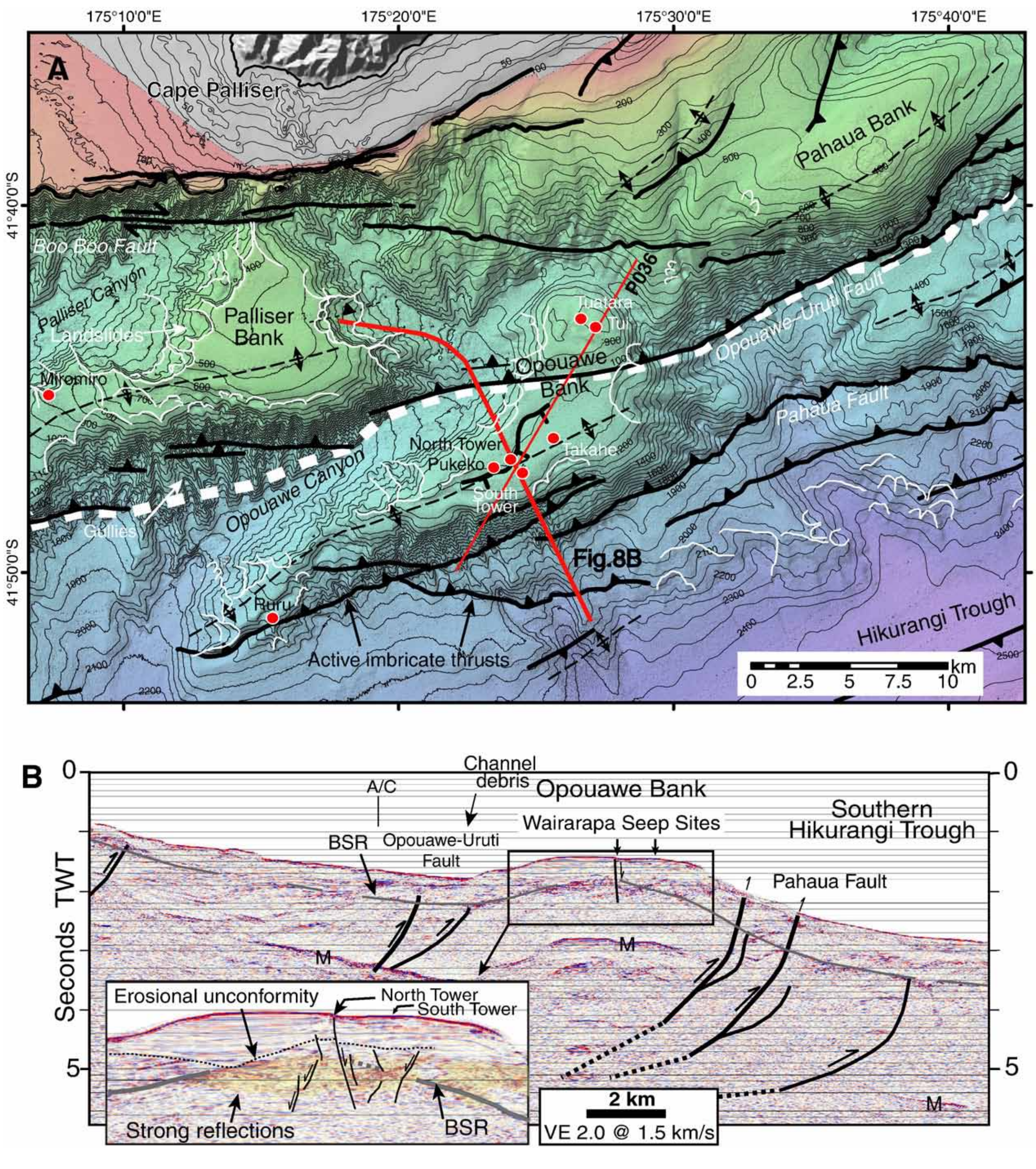

Fig. 8. A. Major tectonic and geomorphic features associated with the Wairarapa seep sites. Bathymetry is 25 m binned, *RV TANGAROA* SIMRAD EM300 multibeam data, with 50 m contour interval. Red dots with white labels are seep sites. The fine white lines indicate major landslide scars. The bold white dashed line is inferred to be the rear of the late Cenozoic accretionary wedge. Pahaua Bank is an informal name used by Mountjoy et al. (2009). Map location is shown in Fig. 1. B. Multichannel seismic section SO191#9/10 revealing structures beneath Opouawe Bank. Yellow shading on seismic zoom indicates packages of high-amplitude reflections beneath seeps.

Paleogene inner foundation rocks underlie Palliser and Pahaua banks, and the upper part of Opouawe Bank, based on correlation of major thrust faults along the margin (Fig. 8A). This foundation was previously considered to extend further seaward beneath the lower part of Opouawe Bank (Barnes and Mercier de Lépinay, 1997). Beneath Opouawe Bank, the upper 0.5 s TWT (c. 440 m) sequence appears to be part of the slope sediment cover, in which there is at least one erosional unconformity (Fig. 8B). Below a packet of strong reflections, the stratigraphy is not clear, but is inferred to include accreted trench turbidites. Therefore the interpreted boundary is tentatively moved to the Opouawe–Uruti Fault.

The seismic data show that a strong and continuous BSR underlies the flanks of Opouawe Bank (Fig. 8B). The BSR shallows from about 0.7 s TWT below the seafloor south of the bank to about 0.35 s TWT (c. 300 m) beneath the crest, and appears to become disrupted in a stratigraphic interval characterized by strong discontinuous reflectors, shallow normal faults, and gas chimneys (Netzeband et al., 2010-this issue). The largest normal fault displaces the seabed at North Tower seep site. Netzeband et al. (2010-this issue) interpreted the strong reflections as evidence of free gas, and the steep faults to penetrate the base of the gas hydrate stability zone. The seep sites are characterized by anomalous resistivities indicative of large amounts of gas or gas hydrate beneath them (Schwalenberg et al., 2010-this issue), hydroacoustic flares (Greinert et al., 2010-this issue), and carbonate mounds and seep faunas (Klaucke et al., 2010-this issue; Naudts et al., 2010-this issue).

4.2. Uruti Ridge sites

Uruti Ridge lies on the middle slope off the Wairarapa coast, where the offshore part of the imbricate wedge is about 90 km wide (Figs. 1 and 2A). The ridge is an anticlinal structural high with bathymetric relief of about 1000 m. A seismic profile presented by Barnes et al. (1998a, their Fig. 5C) reveals the ridge is underlain by the northern part of the Opouawe–Uruti thrust, which breaks out at the toe of the steep, landslide scarred forelimb flank (Fig. 9A). The ridge is dissected by an E–W striking, strike-slip fault, considered by Barnes et al. (1998a) as the northern part of the Palliser–Kaiwhata Fault (Figs. 2 and 9). The latter structure is steeply dipping, and is associated with a small pull-apart basin developed at a releasing bend in the centre of the ridge. There are a number of extensional splay faults on the steep forelimb of the ridge, where the fault intersects the Opouawe–Uruti thrust (Fig. 9B and C). Based on EM300 multibeam bathymetry data, the crest of the ridge, and both its flanks, appear to be dextrally displaced by perhaps 1.0–1.5 km. It is not clear from the data whether the northern end of the Palliser–Kaiwhata Fault penetrates deep into the imbricate wedge, or is confined to the hanging wall of the Opouawe–Uruti thrust.

Dated samples T119 and V479 dredged from the steep forelimb of the ridge (Fig. 9A and B) indicate that the sequence in the hanging wall of the Opouawe–Uruti thrust includes indurated mudstone of Early to middle Pliocene age (see Electronic Data Supplement and Fig. 5 profile C of Barnes et al., 1998a). Above these strata, younger sediments of the Uruti Basin sequence thin towards the ridge crest, having been deposited contemporaneously with uplift of the ridge. Below them, the foundation of the ridge is thought to consist of pre-subduction, passive margin Cretaceous and Paleogene rocks (Lewis et al., 1999).

Three seep sites, including LM-10, Hihi, and Kereru are located at small mounds on the anticlinal crest of the ridge in about 800 m water depth (Fig. 9A). These sites lie about 700–1100 m south of the Palliser–Kaiwhata fault. Projecting sample T119 onto profile P041 (Fig. 9B) indicates that strata on the ridge crest in the vicinity of the seep sites are likely to be of Pliocene age. A BSR is imaged beneath the ridge, rising slightly to ~0.28 s TWT depth beneath the seep sites. The seep sites themselves are characterized by strong backscatter in sidescan sonar images, prolonged echos in 2–10 kHz Chirp profiles, and acoustic flares in the water column (Greinert et al., 2010-this issue).

4.3. Omakere Ridge sites

Omakere Ridge is one of the many slope parallel thrust-faulted anticlinal ridges that characterize the wider part of the Hikurangi Margin off southern Hawkes Bay (Figs. 1 and 2A). The ridge lies in about 1100 m water depth, and has about 500 m of bathymetric relief (Fig. 10B). Its morphology is heavily scarred by landslides, which are particularly common on the steep forelimb flank. The variable subsurface structure of the ridge is illustrated in three seismic reflection profiles from the southern (Fig. 3), central (Fig. 10C) and northern (Figs. 4 and 10A) areas of the ridge. The main active trace of the Omakere Ridge thrust breaks out at the seabed at the toe of the steep seaward flank. The profiles reveal that inactive imbricate thrusts lie below this structure, their tips now buried by sediments in Paoanui Trough. A second active imbricate thrust branches upwards through the hanging wall sequence of the main fault. This structure breaks out at the seabed along the crest of the ridge, where a scarp about 100 m high is associated with a series of discontinuous basins. Based on the change in seismic characteristics of the thrust wedge across Paoanui and Porangahau ridges further seawards (Figs. 2A, 3 and 5), and a Late Cretaceous rock sample dredged from the western flank of Ritchie Ridge (Figs. 1 and 2B) (see also sample T109 projected onto Fig. 4) (Lewis and Marshall, 1996), the thrust wedge beneath Omakere Ridge is interpreted to comprise imbricated Cretaceous and Paleogene rocks lying landward of the accreted trench-fill turbidites (Fig. 3). These rocks are covered by about 0.8 s TWT (700–800 m) of slope sediments that have been folded in the hanging wall of the lower thrust faults.

Several seep sites are recognized on the crest of the ridge, typically in about 1100–1500 m water depth (Jones et al., 2010-this issue; Greinert et al., 2010-this issue). These include LM-9 and Bear's Paw (we are not sure if Moa is a seep site, it might be an inactive one) on the hanging wall of the main Omakere Ridge thrust, as well as Kaka, Kea and Kakapo lying above the upper imbricate thrust (Fig. 10B). They are characterized by methane rich fluid seepage, acoustic flares, authigenic carbonate forming meter high chemoherm structures, and seep fauna (Jones et al., 2010-this issue). At LM-9 a BSR is visible under the seaward flank of the ridge (Fig. 10C), but not directly beneath the crest. In the latter area reflections are disturbed by a shallow extensional fault array and by apparent gas masking. North of the seep sites, the BSR is particularly strong beneath the ridge crest on GECO RESOLUTION NIGHT profile (Fig. 10A).

4.4. Rock Garden sites

The surface of Rock Garden lies in about 600–800 m water depth. The anomalous bathymetric elevation and complex tectonic history of this area and Ritchie Ridge further to the north (Figs. 10B and 11), relative to structural ridges in a comparable position in the outer margin south of Rock Garden, reflects the enhanced uplift and deformation of these features above positive relief on the subducted Pacific Plate (Fig. 4) (refer to Section 3.2 above). Based on the seismic reflection characteristics beneath the ridge (Fig. 7), and rock samples of Late Cretaceous age from the southwestern part of Ritchie Ridge some 30 km to the north (Lewis and Marshall, 1996, sample T109), it is likely that at least the western crest and flank of Rock Garden is cored by the Cretaceous and Paleogene rocks (Fig. 4). The outer flank of Rock Garden is interpreted here to be cored by accreted turbidites, however the surface and subsurface stratigraphy over the outer crest remains uncertain. The flanks of Rock Garden, particularly in the south, are characterized by numerous landslide scars (Fig. 10B) (Faure et al., 2006).

The plateau-like crest of Rock Garden is eroded, and strongly reflective (Fig. 7) (Lewis and Marshall, 1996). Beneath the surface is a discontinuous BSR and packages of high-amplitude reflections that have been interpreted by Pecher (2002), Pecher et al. (2004) and Crutchley et al. (2010-this issue) as gas migration pathways. The BSR is generally strong beneath the seaward flank, and locally pinches out at the edges of the plateau. Pecher et al. (2005) suggested that the erosion of the ridge crest is linked

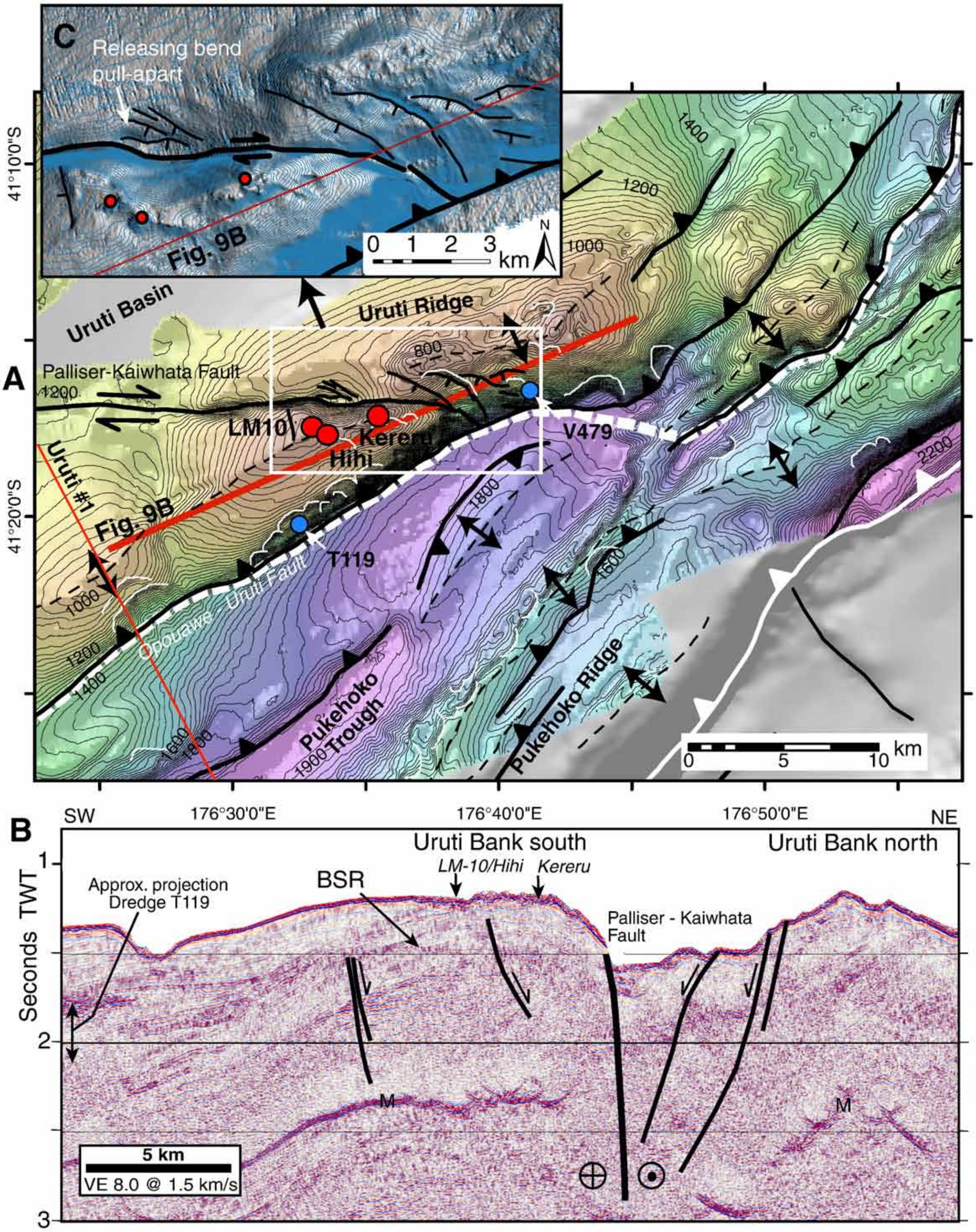

Fig. 9. Major tectonic and bathymetric features associated with the Uruti Ridge seep sites. A. Regional map with stretched colour DTM on 150 m grid multibeam bathymetry data acquired on *RV TANGAROA* and *SONNE*, and 20 m contour interval. Grey area is a background hillshade from archived SIMRAD EM12 Dual multibeam data acquired by *RV L'ATALANTE*. The profile labeled Uruti#1 is illustrated in Fig. 5C of Barnes et al. (1998a). The bold dashed white line is inferred to be the back of the late Cenozoic accretionary wedge. See Figs. 1 and 2 for location of map. Red dots are seep sites. B. High-resolution multichannel seismic section SO191#P041 illustrating structure of the eastern end of the Palliser–Kaiwhata Fault. M is the first seafloor multiple. Note the major seaward-vergent thrust fault beneath the ridge is not imaged in this profile. C. Zoom map of structure and bathymetry based on a 25 m grid hillshade with 5× vertical exaggeration from *RV TANGAROA* SIMRAD EM300 data.

primarily to temperature-controlled fluctuations in the stability of gas hydrate. Recent modelling by Ellis et al. (2010-this issue), indicates erosion of the ridge top likely relates to interactions between tectonic uplift caused by seamount subduction, and the stability of shallow gas hydrates.

Seep sites have been recognized in four areas on Rock Garden (Figs. 7A and 10B) (Lewis and Marshall, 1996; Faure et al., 2006; Greinert et al., 2010-this issue; Crutchley et al., 2010-this issue). These sites, including LM-3, Weka, Faure's Site, and Rock Garden Knoll, are associated with seep faunas, methane-derived carbonates and acoustic water column flares that have been proven to be caused by methane bubbles (Faure et al., 2010-this issue; Naudts et al., 2010-this issue). All sites lie on the hanging wall, and within 1.2 km of the surface trace of a major NE–SW striking, seaward-vergent thrust fault that has displaced the top of the bank. In addition, Faure's Sites are associated with the headwall scarp of a large, deep seated landslide on the southern flank of the bank (Fig. 7A and B) (Faure et al., 2006).

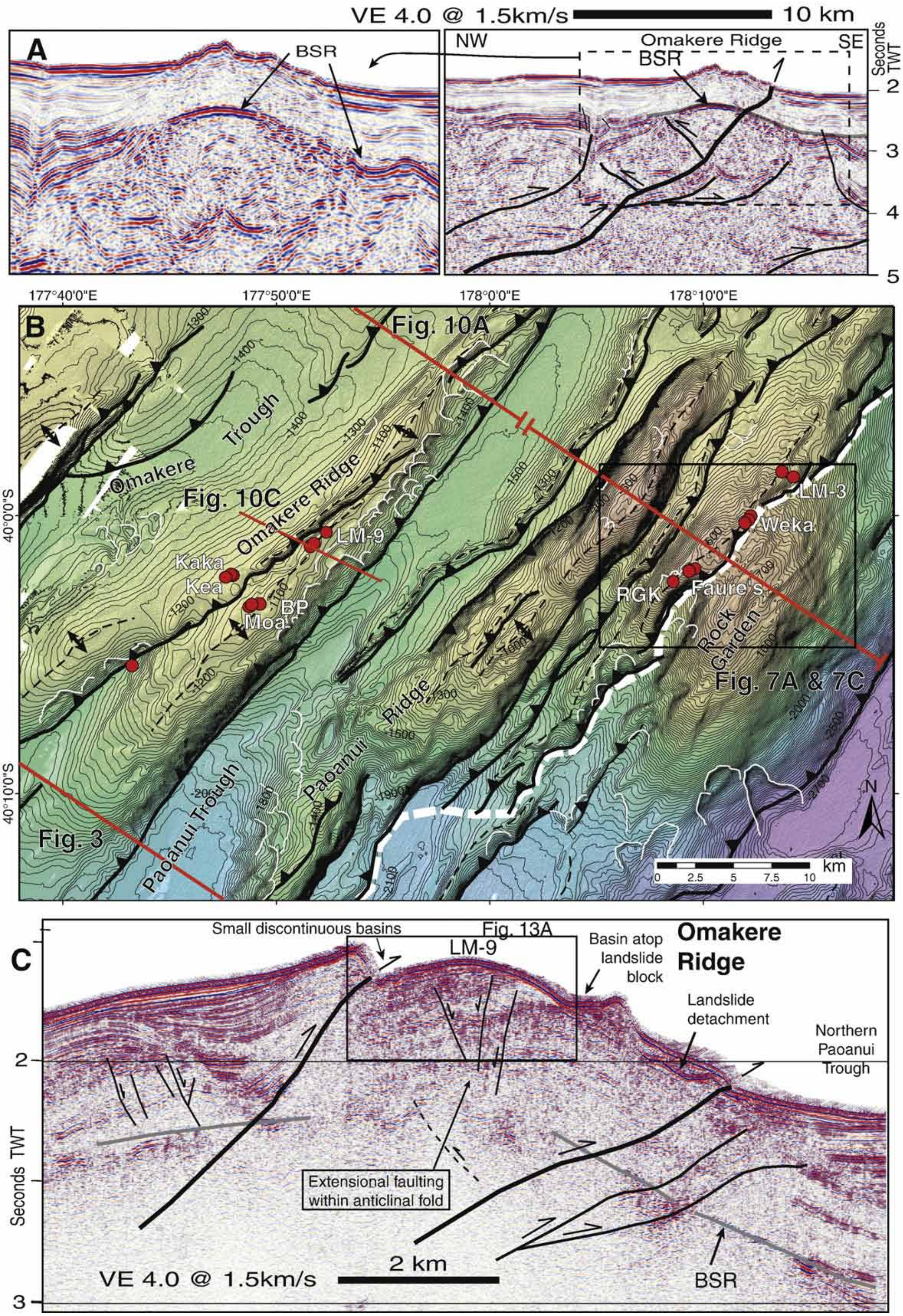

Fig. 10. Major tectonic and bathymetric features associated with the Omakere Ridge and Rock Garden seep sites. A. Uninterpreted zoom and interpreted high-fold NIGHT seismic data across Omakere Ridge. B. Structure map with 30 m grid multibeam bathymetry data acquired on *RV TANGAROA* and *SONNE*, and 20 m contour interval. Red dots are seep sites (Abbreviation RGK is Rock Garden Knoll). The bold dashed white line is inferred to be the back of the late Cenozoic accretionary wedge. See Figs. 1 and 2A for map location. C. High-resolution multichannel seismic section SO191#P054 indicating major structures beneath LM-9.

4.5. Builders Pencil (Ritchie Ridge) sites

The Builders Pencil and LM-1 seep sites lie on the landward flank of Ritchie Ridge, which is located in the middle slope region about 50 km southeast of Mahia Peninsula (Figs. 1 and 11) (Lewis and Marshall, 1996; Greinert et al., 2010-this issue). On the ridge crest are Ritchie, Calyptogena, and Pantin banks, rising to about 300 m, 850 m, and 1050 m, respectively. The ridge is underlain by an anticline above an active thrust fault. This fault is the first major active upper plate structure east of the Lachlan Fault, which lies beneath the inner shelf >30 km to the west (Fig. 11A) (Barnes et al., 2002). The fault ramps off the plate interface and splays upwards into 2–3 imbricates which break out at the seabed across the seaward flank of the ridge (Fig. 11B). Inactive backthrusts are observed off the upper imbricate.

The spliced seismic profiles in Fig. 11B illustrate that the Ritchie Ridge thrust transports previously imbricated Cretaceous and Paleogene foundation rocks, and their overlying slope basin sequence, over

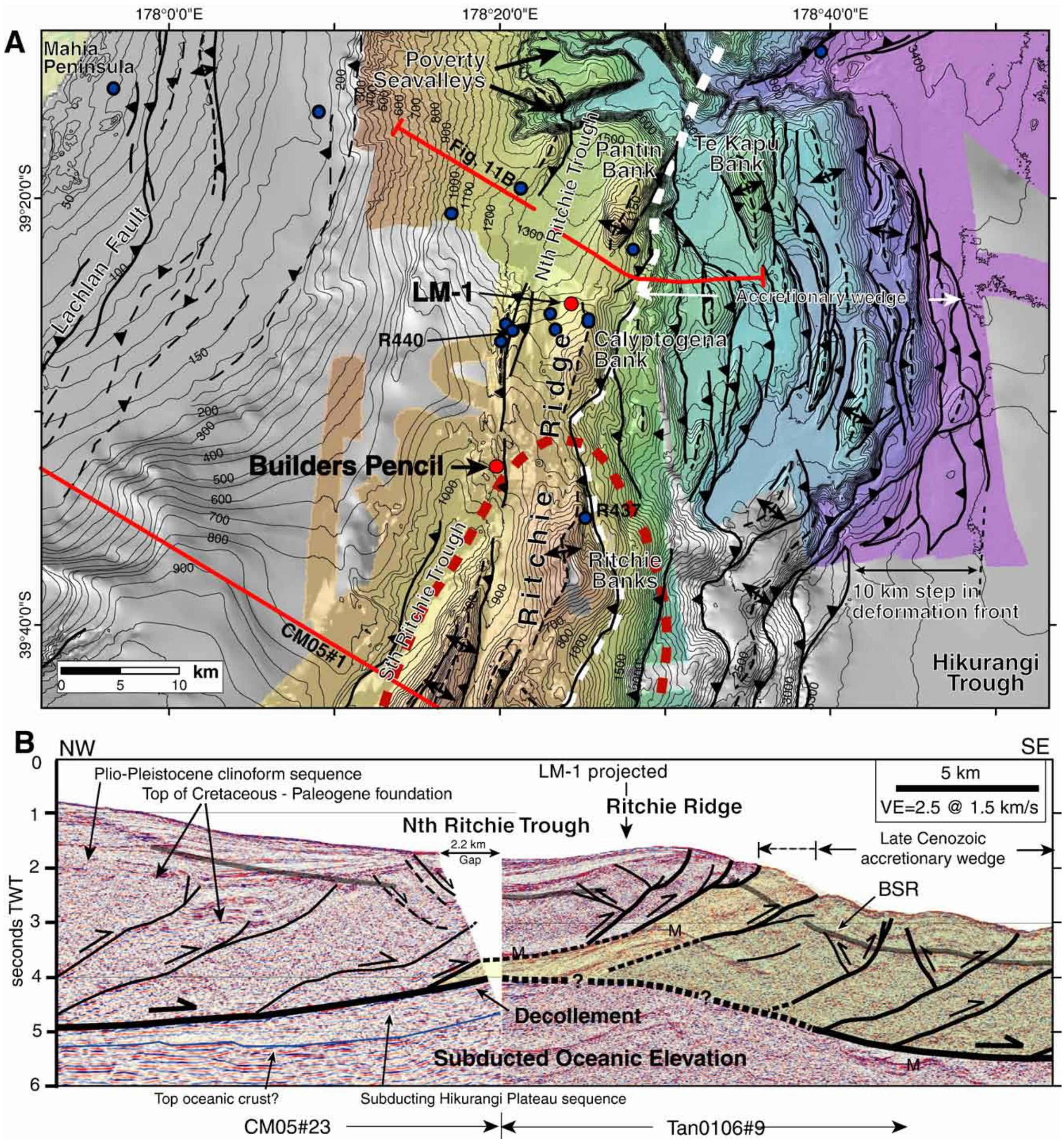

Fig. 11. Major tectonic and bathymetric features associated with the Builders Pencil and LM-1 seep sites off Mahia Peninsula. A. Regional map has stretched colour DTM on 25 m binned, *RV TANGAROA* SIMRAD EM300 multibeam data and 30 m grid *RV SONNE* EM120 multibeam. Contour interval is 50 m. Grey area is a background hillshade from archived SIMRAD EM12 Dual multibeam data acquired by *RV L'ATALANTE*, and coastal echosoundings. See Fig. 1 for map location. The bold dashed white line is inferred to be the back of the late Cenozoic accretionary wedge. The bold dashed red line is the inferred extent of high relief on the subducting Pacific Plate (see southern part of this feature beneath the Rock Garden in Fig. 2A, where it is highlighted in yellow). Red dots are seep sites. Blue dots are dredge sites from NIWA's database. B. Spliced multichannel seismic section including high-fold CM05#23 and low-fold Tan0106#9 data, revealing major structures beneath Ritchie Ridge. The green shading is the extent of the accreted trench-fill turbidites (yellow shading indicates region of compositional uncertainty at the rear of the frontal wedge).

accreted trench turbidites beneath the seaward flank of the ridge. The accreted trench sequence is highly imbricated and covered by thin slope basin sediments. The older foundation rocks landward have been dredged from the seafloor near the coast west of the Lachlan Fault (Barnes et al., 2002), and at Ritchie Banks, where hard massive siltstone of possible mid Eocene–E. Miocene age has been recovered at station R437 (Fig. 11) (A. Edwards, pers. comm, 1991). Middle Miocene strata overlying these rocks were recovered from a structural high on the western edge of Ritchie Ridge (station R440) about 5 km west of LM-1 (Lewis and Marshall, 1996). The upper part of the cover sequence west of Ritchie Ridge is part of a classical Plio-Pleistocene shelf–slope clinoform succession that is well developed off eastern Mahia Peninsula. This sequence thins onto the back of Ritchie Ridge and is being actively uplifted and folded.

The Builders Pencil and LM-1 sites lie in about 850–1200 m water depth, are characterized by widespread relict seep faunas, and appear to be presently inactive (Lewis and Marshall, 1996; Greinert et al., 2010-this issue). Greinert et al. (2010-this issue) demonstrate that the seafloor surrounding the sites is characterized by tilted, highly eroded and exposed bedrock sequences. Considering the seismic stratigraphy and structure outlined above, we infer this sequence on the backlimb of the ridge is Miocene and/or Pliocene age.

5. Discussion

5.1. Comparison of seep site settings

The five areas of seeps described above represent a variety of different local geological settings within the imbricate thrust wedge, but they also have some important similarities. All sites lie on the crests of seaward-vergent, thrust-faulted ridges, none lie in slope basins between thrust ridges. The locations therefore differ from some relict early Miocene seeps documented in uplifted forearc basins on land (Campbell et al., 2008). The Uruti Ridge sites are unusual in that they also lie in close proximity to the eastern end of a major strike-slip fault. Rock Garden sites differ from others to the south in that they occur directly above a substantial seamount that is currently being subducted. Greinert et al. (2010-this issue) demonstrate that the Wairarapa, Uruti Ridge, Omakere Ridge and Rock Garden seeps are currently active, whereas Builders Pencil appears to be relict of a very active earlier phase.

Another important similarity between all confirmed seep sites is that they lie approximately along the middle slope, commonly in about 700–1200 m water depth, near the outer edge of the deforming Cretaceous and Paleogene foundation rocks (Figs. 1 and 12A) (Lewis and Marshall, 1996). The Uruti Ridge, Rock Garden, and Builders Pencil sites all occur on ridges directly above the outer edge of the Cretaceous and Paleogene foundation (Figs. 2A, 4, 9–11). The southern Wairarapa sites, Omakere Ridge, and the southern Porangahau Ridge investigated by Pecher et al. (2010-this issue), lie within one ridge either side of this buttress (Figs. 1–3 and 8). These seep locations collectively indicate that the imbricated Cretaceous and Paleogene foundation rocks play an important role in focusing present fluid flow and seepage along the middle part of the margin (see discussion in Section 5.3).

The shallow seismic stratigraphy of the different seep areas appears to vary greatly, but has not been accurately dated at the specific seep sites. Consideration of regional seismic reflection characteristics and sparse seafloor samples leads us to infer that the Wairarapa and Omakere Ridge seeps are located on late Pleistocene slope sediments. At Uruti Ridge they are developed on probable Pliocene strata which are exposed at the crest and seaward flank of the ridge. The Builders Pencil substrate appears to be Miocene and/or Pliocene strata, which overlie older rocks exposed on the seaward flank of Ritchie Ridge. The Rock Garden seeps, located on the western side of Rock Garden, may lie on a substrate of exposed Cretaceous and Paleogene rocks, or on an eroded cover sequence of Miocene–Pliocene age.

5.2. New insights into the structure of the Hikurangi Margin

Whilst to a first order, the major tectonic and stratigraphic attributes of the central Hikurangi Margin were established previously (Davey et al., 1986a,b; Lewis and Pettinga, 1993; Collot et al., 1996; Barnes and Mercier de Lépinay, 1997; Lewis et al., 1997, 1999; Field et al., 1997; Barnes et al., 1998a,b; Henrys et al., 2006; Nicol et al., 2007), we make five significant contributions in this study. These are (1) improved mapping of the major structures within the margin based on wider seismic reflection coverage, including high-fold deep penetration datasets, and higher resolution multibeam bathymetry data (e.g., Fig. 2); (2) improved definition of the subducting seamounts at Rock Garden (Figs. 4, 7, and 10B) and Bennett Knoll (Fig. 6A), and better understanding of the tectonic responses of the margin to seamount subduction; (3) improved geophysical clarity and revised mapping of the contact between the imbricated Cretaceous–Paleogene inner foundation rocks and the late Cenozoic frontal wedge of accreted trench-fill turbidites (e.g., Figs. 2A and 5); (4) improved seismic stratigraphy of the subducting and accreting sedimentary sequences in the Hikurangi Trough, and clearer identification of the interplate décollement within the pelagic sequence (e.g., Fig. 6B); and (5) improved seismic imaging and wider mapping of the protothrust zone (Figs. 2A and 6B).

At up to 150 km in width, the imbricated frontal wedge of the central Hikurangi Margin is considered to be a wide subduction margin (c.f., von Huene and Scholl, 1991). Its tectonic structure, morphology, and inferred hydrogeological system, summarized in Fig. 12A, are characteristic of wide, low taper thrust wedges associated with relatively smooth subducting plate, thick trench-fill sedimentary sequence, and moderate convergence rate. The low taper (~4°) of the wedge, with average surface slope of about 1°, is low by comparison with many subduction systems (Davis et al., 1983; Lallemand et al., 1994). This taper is typical of poorly drained, low permeability thrust wedges (Saffer and Bekins, 2002) with substantial fluids channeled along a weak basal décollement (Moore et al., 1995; Bangs et al., 1999, 2004; Brown et al., 2003; Lamb, 2006; Morgan et al., 2007; Saffer, 2007). It is also consistent with high fluid pressures approaching lithostatic overburden encountered in exploration wells from the upper Hikurangi Margin (Davies et al., 2000; Darby et al., 2000), and interpreted in the frontal parts of similar thrust systems (e.g., Maltman et al., 1993; Tobin et al., 1994; Moore and Saffer, 2001; Saffer, 2003, 2007).

One of the possible effects of rapid frontal accretion is to lower the taper of a thrust wedge. This may produce a mechanical response, whereby out-of-sequence thrusting behind the propagating deformation front leads to thickening of the rear and middle parts of the wedge in order to maintain a critical taper (e.g., Davis et al., 1983; Lallemand et al., 1994). Out of sequence thrusts are active across the upper and middle parts of the central Hikurangi Margin. These include reactivated Miocene thrust systems such as Motuokura Ridge (Figs. 3 and 12B), Lachlan Ridge (Fig. 1B) (Barnes et al., 2002), and Kidnappers Ridge (Barnes and Nicol, 2004), and reactivated thrusts presently inverting mid-slope basins (e.g., Fig. 5) (Davey et al., 1986a; Lewis and Pettinga, 1993; Barnes and Mercier de Lépinay, 1997). Similar out-of-sequence thrusting has been recognized at a number of other subduction margins (Moore et al., 2007).

The classical accretionary wedge of the central Hikurangi Margin contrasts strongly with the narrower and steeper northern margin, the latter of which is representative of subduction systems characterized by relatively thin (~1 km) trench-fill sequence, high relief (~1–3 km) on the subducting plate, relatively rapid convergence rate (~45–58 mm/yr), and non-accretion and/or frontal tectonic erosion processes (Von Huene and Lallemand, 1990; von Huene and Scholl,

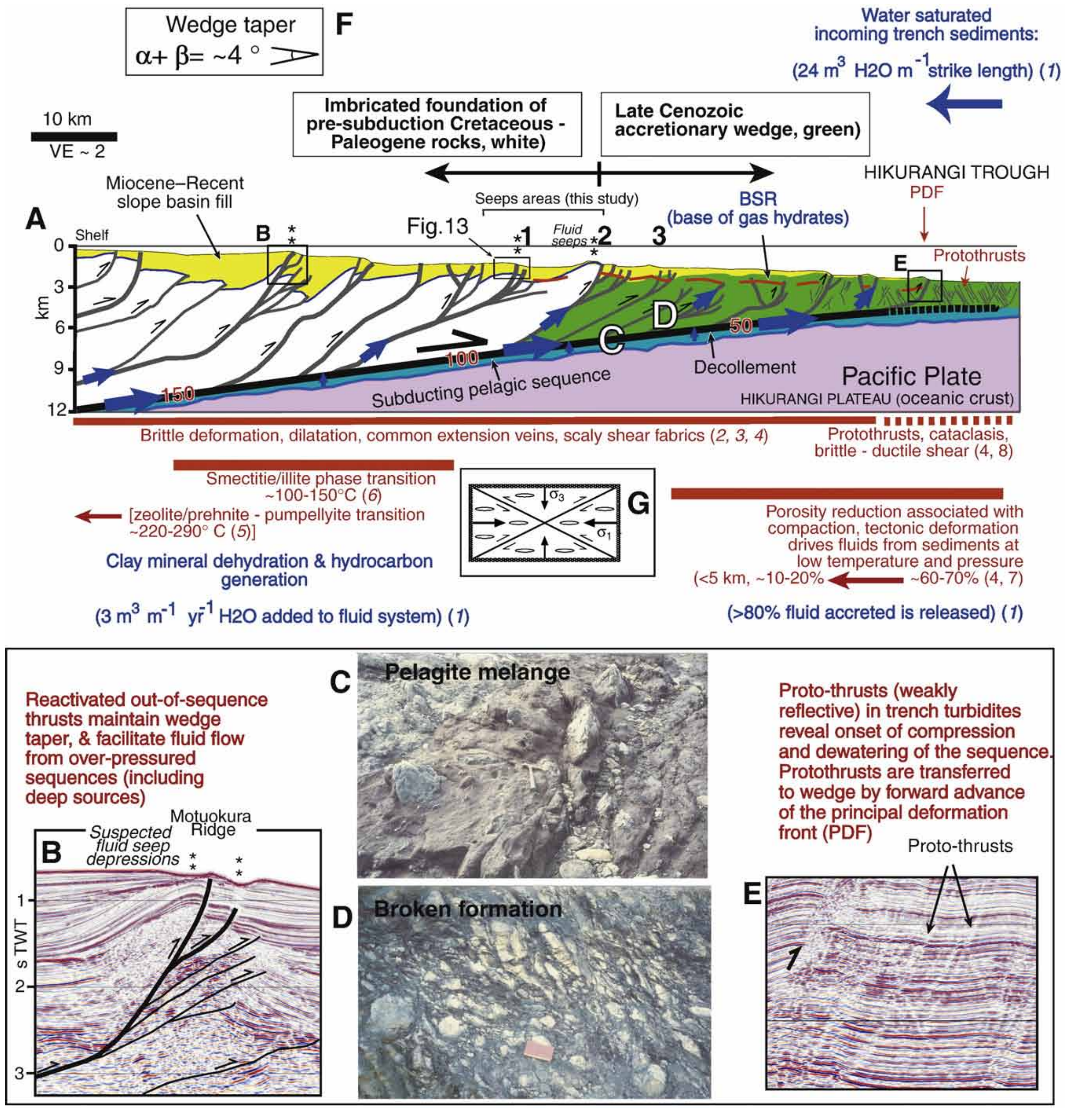

Fig. 12. Summary of tectonic, stratigraphic, and hydrogeological aspects of the Hikurangi Margin imbricate thrust wedge. A. Cross-section of the offshore margin 35 km south of Rock Garden, at ~2× vertical exaggeration, based in Fig. 3. Depth to plate interface is based in Fig. 4 inset, and data from Davey et al. (1986a), Henrys et al. (2006), and Nicol et al. (2007). Bold numbers above the cross-section refer to the indicative locations of the seep sites discussed in this paper, whereby: (1) includes Omakere Ridge (Figs. 2 and 10); (2) includes Palliser Bank and upper Opouawe Bank (Wairarapa sites, Figs. 1 and 8), Uruti Ridge (Figs. 2 and 9), Rock Garden (Figs. 2, 4 and 10), and Builders Pencil (Ritchie Ridge) (Figs. 1 and 11); and (3) includes lower Opouawe Bank (Fig. 8). Porangahau Ridge, studied by Pecher et al. (2010-this issue), is also represented by location 3. Text in blue (1) concerns the fluid budget, with estimates from Townend (1997a). Bold blue arrows illustrate primary fluid flow along décollement and thrust splay faults. Bold red numbers along the décollement are estimates of temperature in °C at the interplate thrust (McCaffrey et al., 2008). Selected references for deformation fabrics and mineral phase changes include: 2, Bryne and Fisher (1990); 3, Maltman et al. (1993); 4, Morgan et al. (2007); 5, Ernst (1990); 6, Vrolijk (1990); 7, Moore (1989); 8, Morgan and Karig (1995). B. High-fold multichannel seismic section CM05#30 illustrating thrust imbricates beneath suspected seeps sites on the southern Motuokura Ridge. The profile is projected 11 km onto cross-section A, whilst its actual location is shown in Fig. 2A. C and D illustrate what is interpreted to be analogous field examples of low *P*–*T* accretionary deformation fabrics from 100 Myr old subduction complex exposed in south eastern Wairarapa (Barnes and Korsch, 1991). C, tectonic mélange with pelagite matrix and "exotic" oceanic floaters; D, broken formation developed in turbidites. E. Zoom of seismic section SO191#6 (Fig. 6B) illustrating protothrusts at the deformation front. F. Thrust wedge taper where α and β are the surface slope and décollement dip, respectively. G. Schematic of thrusts and dilatational fractures developing in relation to maximum and minimum axes of principal compression (e.g., Sibson, 1992).

1991). The transition between these two present segments of the margin can now be located with greater confidence at the southern end of Rock Garden (Figs. 1B and 2B). The substantial relief (~3 km) associated with the seamount subducted beneath Rock Garden can be inferred to extend at least as far north as Ritchie Banks, based on its similarly high bathymetric elevation, and lies west of a 10 km-wide right step in the line of the deformation front at about 39 35′S (Fig. 11A).

5.3. The role of faulting in fluid migration and expulsion

Subduction systems associated with thick trench sequences have dynamic fluid systems because accreting and subducting sediments dewater in response to compaction and contractional deformation (e.g., Fig. 12A) (Moore, 1989; Moore and Vrolijk, 1992; Morgan et al., 2007). Water saturated trench sediments entering accretionary wedges undergo a change of stress regime, from one where the gravitational load dominates in the trench sequence as it approaches the deformation front, to one where the principal compressive stress approaches horizontal within the accretionary wedge (e.g., Davis et al., 1983). The latter produces structural permeability which facilitates lateral fluid flow (Fig. 12G) (Sibson and Roland, 2003; Saffer, 2007). Fluid flow in thrust fault zones has been reported widely from field observations (e.g., Sibson, 1992), as well as from geophysical and borehole evidence from subduction margins (e.g., Moore et al., 1986; LePichon et al., 1990; Taira et al., 1992; Tobin et al., 1994; Moore et al., 1995; 2004., Bangs et al., 1999, 2004). Field studies of ancient accretionary rocks (e.g., Moore and Wheeler, 1978; Cowan, 1982) and Ocean Drilling Project cores (e.g., Maltman et al., 1993; Morgan and Karig, 1995) show that a turbidite sequence entering an accretionary wedge undergoes substantial (c. 30–40%) porosity reduction and consolidation associated with deformation under low confining pressure and temperature, but high strain rates. Within the frontal part of the wedge, localized ductile flow, cataclasis, kink band development, and brittle faulting typically produces stratal disruption fabrics from previously coherent sequences, at up to kilometer scale (e.g., Fig. 12D) (e.g., Moore, 1989; Karig and Lundberg, 1990; Barnes and Korsch, 1991; Moore and Vrolijk, 1992; Maltman et al., 1993; Morgan and Karig, 1995; Morgan et al., 2007). Complex vein arrays in disrupted sequences referred to as broken formation, indicate that brittle faulting and fractures facilitate fluid flow by creating structural permeability (Moore and Byrne, 1987). Mesoscale broken formation is inferred to exist in the frontal wedge of the Hikurangi Margin, particularly in proximity to the major seismically imaged thrust faults (Lewis and Marshall, 1996; Barnes and Mercier de Lépinay, 1997). Such deformation fabrics, together with steep bedding dips and shallow gas, may contribute to loss of seismic reflection character commonly observed in the vicinity of the major faults (e.g., Fig. 12B and E) (Crutchley et al., 2010-this issue; Pecher et al., 2010-this issue).

The décollement beneath the frontal wedge of the central Hikurangi Margin is inferred to be located within the pelagic sediments (nannofossil chalks, tephras, mudstone, clays) of the Hikurangi Plateau sequence (Fig. 6B). Based on ocean drilling of other margins (Maltman et al., 1993; Morgan et al., 2007), and field examples of ancient analogues (Barnes and Korsch, 1991), the décollement deformation zone may be tens of meters in thickness, and have an internal structure resembling the Cretaceous mélange illustrated in Fig. 12C. The low pressure and temperature (zeolite facies) analogue field example in Fig. 12C is characterized by a pervasively sheared matrix of pelagite mudstone containing sheared blocks of greywacke from the upper plate, together with basalt and chert blocks from the oceanic lower plate.

To date, acoustic flares indicative of active fluid/gas venting have not been identified beneath the lower continental slope of the Hikurangi Margin (Lewis and Marshall, 1996; Greinert et al., 2010-this issue). Three lines of evidence, however, indicate that the frontal wedge is dewatering seaward of where the active seep sites are located. Firstly the presence of a gas hydrate BSR extending across the frontal wedge essentially to the deformation front indicates rising gas-charged fluids (Figs. 3, 4, 6, 8B, 11B) (Lewis and Marshall, 1996; Henrys et al., 2003). Secondly, there is an extraordinarily large (200 km length by 20 km width) protothrust zone beyond the principal deformation front in the Hikurangi Trough (Figs. 2A, 6B, 12A and E). Such incipient thrusts, and/or mega-kink bands characterized by relatively weak reflectivity, are commonly interpreted as dewatering conduits above the tip of the interplate thrust where it is propagating into the trench sequence (e.g., Moore et al., 1986, 1995; Platt, 1990; Morgan and Karig, 1995; Barnes and Mercier de Lépinay, 1997). Thirdly, two unconfirmed sites of suspected former fluid seepage are inferred on lower slope thrust ridges, from Hawaii MR1 sidescan sonar images (Fig. 2). One site (Fig. 2D) is a possible mud volcano (Barnes and Mercier de Lépinay, 1997), the other appears to be an edifice surrounded by radiating mud flow deposits (Fig. 2C). Whilst it is apparent that the frontal wedge is dewatering, its relative volumetric contribution to the total fluid release estimated from the margin is very poorly constrained (Townend, 1997a).

There is a clear relationship between the mid-slope line of confirmed fluid seep sites and major thrust faults near the outer edge of the Cretaceous and Paleogene foundation rocks (Figs. 1 and 12A) (Lewis and Marshall, 1996). Only one submarine site of suspected (i.e., unconfirmed) fluid seepage is recognized well inboard (~50 km) of this mid-slope buttress, on Motuokura Ridge (Figs. 2A, 12A and B). The major thrust faults beneath the active seeps are seaward-vergent and inferred to be primary fluid conduits (Fig. 13). The source of the fluids tapped by these faults must therefore be largely landward of the seep sites. These source rocks potentially include the Cretaceous and Paleogene sequences, the innermost (landward) part of the late Cenozoic frontal accretionary wedge, and sediments subducted and possibly underplated at depths of >9 km beneath the inner foundation or basement backstop of the margin (Barker et al., 2009). Estimates of temperatures at the Hikurangi interplate thrust indicate that offshore deformation and fluid expulsion is occurring at <150 °C (Fig. 12A) (McCaffrey et al., 2008). The fluids that supply onland seeps and overpressured stratigraphic intervals encountered in exploration wells near the coast are generally considered to have been sourced from the imbricated Cretaceous and Paleogene foundation rocks at depths of <5–6 km (Ridd, 1970, Kvenvolden and Pettinga, 1989; Lewis and Marshall 1996; Field et al., 1997; Davies et al., 2000; Darby et al., 2000; Pettinga, 2003; Uruski et al., 2004).

We consider that the apparent concentration of active submarine fluid seeps above the outer edge of the Cretaceous–Paleogene foundation, reflects the overall poor permeability of this unit, and the migration of fluids being channeled eastwards along the interplate décollement and on major low-angle thrust splay faults towards its outer edge (Fig. 12A) (cf. Lewis and Marshall, 1996). The low permeability of the Cretaceous–Paleogene foundation is consistent with (1) fluid pressures approaching lithostatic overburden encountered in east coast exploration wells, which have been shown to relate to low permeability mudstones with high smectite contents in the Cretaceous–Paleogene sequence (Darby et al., 2000; Darby, 2002), and (2) presence of former low-angle detachments associated with listric faulting in the upper margin, which have been inferred to be rooted in weak mudstone-rich stratigraphic intervals within the sequence (Barnes and Nicol, 2004).

Any fluids sourced from subducted sediments beneath the inner margin must firstly enter the décollement zone, and later the thrust wedge. Fluid flow into the décollement could potentially be achieved by progressive downward migration of the décollement deformation into the top of the subducting sequence, and/or by increased fluid pressure gradient resulting from temporarily increased permeability in décollement rocks by dilatation of scaly shear fabric during and after décollement rupture (e.g., Moore, 1989; Saffer, 2007). Fluid flow within the décollement may be episodic, associated with fluid pressure cycling produced by fault valve action (Sibson, 1992; Sibson and Roland, 2003). Fluid migration into the upper plate wedge will be enhanced at sites where splay thrusts ramp upward from the décollement.

All of the active fluid seeps recognized on the Hikurangi Margin lie on anticlines developed in the hanging wall of thrust faults (Figs. 12A and 13). Although thrust tips commonly break out at the seabed on the relatively steep forelimb (seaward) side of anticlinal ridges, the seeps are generally on the top of the ridges. Beneath each active seep site, there is a conspicuous break in the BSR, and common occurrence of high-amplitude reflections inferred to result from gas-charged stratigraphic

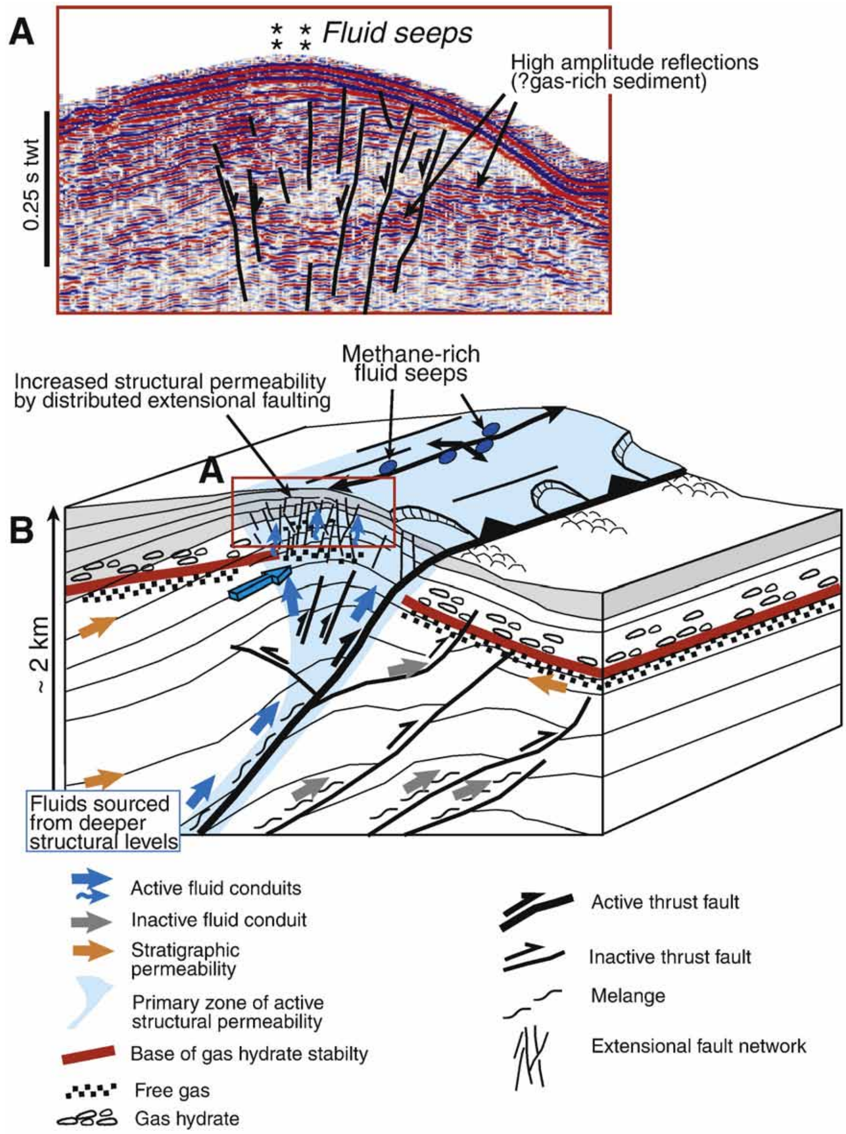

Fig. 13. Illustration of structural and stratigraphic permeability beneath active seep sites on Hikurangi Margin thrust ridges. A. Zoom of seismic section SO191#P054 across seep LM9 on Omakere Ridge (Fig. 10C), illustrating distributed extensional fault network in the shallow core of the anticline above an active thrust fault and beneath the seeps. B. Schematic 3D view of a typical Hikurangi Margin seep site illustrating various relationships.

horizons (Fig. 13). The existence of the fluid seeps and the disrupted BSR indicate that gas hydrates are not a barrier to fluid flow at these sites (e.g., Nimblett and Ruppel, 2003). Seismic sections reveal arrays of distributed shallow faults within the anticlines (see also Pecher et al., 2010-this issue). These shallow faults are commonly normal such as at Omakere Ridge (Fig. 13A) and Wairarapa sites (Netzeband et al., 2010-this issue), but also include backthrusts such as at LM-3, Rock Garden (Crutchley et al., 2010-this issue). Similar extensional fault arrays have been documented in the upper parts of growth folds beneath the NW Borneo margin (Gee et al., 2007). The normal faults, and probable subseismic fractures, in the anticlines may be a response to flexural extension, and/or hydrofracturing related to excessive pore pressures. Fluids rising along the major thrust faults appear to be siphoned off the faults directly into the shallow fault/fracture networks, and to percolate to the seabed on ridge crests (Pecher et al., 2004, 2010-this issue; Netzeband et al., 2010-this issue; Crutchley et al., 2010-this issue). What has sometimes been referred to as diffusive upward fluid flow related to increased stratigraphic permeability beneath ridges (e.g., Taira et al., 1992) may in fact be distributed fluid flow facilitated principally by fault and fracture permeability. Dipping, permeable stratigraphic layers within the hanging wall and footwall sequences of thrust faults are likely to be secondary fluid conduits that also focus fluid flow towards ridge crests (e.g., Langseth and Moore, 1990; Moore et al., 1990; Lewis and Marshall, 1996; Pecher et al., 2004).

6. Conclusions

1. New seismic reflection and multibeam datasets shed new insights into the tectonic structure, stratigraphy, and morphology of the imbricated frontal wedge of the Hikurangi Margin, and enable us to establish the geological framework for each of five areas in which seep sites are investigated and documented elsewhere in this issue. The imbricated wedge, which is up to 150 km in width, includes an inner foundation of deforming Late Cretaceous and Paleogene rocks, an outer wedge of late Cenozoic accreted trench-fill turbidites, and a deforming cover sequence of Miocene to Recent shelf and slope basin sediments. The contact between the inner foundation and the accretionary wedge has been recognized and located to within c. 10 km. The contact is interpreted to be a significant feature with respect to the hydrogeology of the margin, as it appears to control the location of presently active fluid seeps. The frontal accretionary wedge has a maximum width of c. 65–

70 km in the central margin, excluding a 20 km-wide protothrust zone.

2. The tectonic structure and morphology of the central part of the Hikurangi Margin is characteristic of wide, low taper thrust wedges associated with a relatively smooth subducting plate, a thick trench-fill sedimentary sequence, and moderate convergence rate. On the whole, the low taper (~4°) is consistent with the interpretation that the wedge is poorly drained, has low permeability, a weak basal décollement, and high fluid pressures. The protothrust zone in the Hikurangi Trough seaward of the principal deformation front extends along the margin for over 200 km. Its origin is related to incipient deformation and dewatering processes above the propagating décollement. Although part of the Bennett Knoll seamount ridge is presently subducting beneath the deformation front, the morphology of the accretionary wedge indicates that frontal accretion in the centre of the margin has been largely uninhibited for at least 1–2 Myr. Active out-of-sequence thrusting distributed widely across the margin behind the deformation front maintains the wedge taper.
3. Correlation of the seismic stratigraphy of the central Hikurangi Trough with published stratigraphy of the Hikurangi Plateau sedimentary sequence (Davy et al., 2008) constrains the ages and stratigraphy of the Mesozoic and Cenozoic sequence subducting beneath the interplate décollement. This sequence is inferred to include Cretaceous volcaniclastics, pelagic and clastic sedimentary rocks, and Late Cretaceous–Early Oligocene (70–32 Ma) nannofossil chalks with alternating clays. The décollement is developed within the Hikurangi Plateau sequence up to 400–450 m below what are clearly trench turbidites. Its stratigraphic position for at least 30 km down dip coincides primarily with reflection 7, but over lateral distances of 100–150 km, its stratigraphic position varies by up to 300–400 m within 15 km of the deformation front.
4. Offshore of Hawke Bay a substantial seamount with about 3 km of relief has been subducted beneath the lower margin, resulting in uplift and complex superposed deformation of Rock Garden and southern Ritchie Ridge, and a dramatically reduced active frontal wedge. The southern end of Ritchie Ridge therefore marks the transition from the classical accretionary system along the central margin to the narrower and steeper northern margin characterized by high-relief subducting plate, relatively thinner trench-fill sequence, relatively faster convergence rate, and predominantly non-accretion and/or frontal tectonic erosion processes.
5. The five areas of confirmed seep sites documented elsewhere in this issue, referred to as Wairarapa, Uruti Ridge, Omakere Ridge, Rock Garden, and Builders Pencil, typically lie in about 700–1200 m water depth on the crests of thrust-faulted anticlinal ridges along the mid-slope. The Uruti Ridge sites are unusual in that they also lie in close proximity to the eastern end of a strike-slip fault, whereas Rock Garden sites occur directly above a substantial seamount that is currently subducting. The seeps sites are associated with a variety of substrate stratigraphy. There is a clear relationship between the seeps and major seaward-vergent thrust faults near the outer edge of the deforming Cretaceous and Paleogene inner foundation rocks, indicating that thrust faults are primary fluid conduits and that the Cretaceous and Paleogene inner foundation rocks play a role in focusing fluid flow. The source rocks for the fluids expelling at the seeps potentially include the Cretaceous and Paleogene sequences, the innermost (landward) part of the frontal accretionary wedge, and sediments subducted and possibly underplated at depths of >9 km beneath the inner foundation or basement backstop of the margin. We interpret that the Cretaceous and Paleogene inner foundation is, on the whole, relatively impermeable and focuses fluid migration to its outer edge via major low-angle thrust faults and the interplate décollement.
6. Beneath each area of active seep sites there is a conspicuous break in the BSR, and commonly a seismically-resolvable fault-fracture network and gas-charged horizons within the shallow part of the anticlines. Structural permeability is interpreted to be crucial, within the décollement, the major thrust splay faults, and within shallow anticlinal fault networks which siphon fluids from thrust faults and allow vertical percolation to the seafloor on ridge crests. Stratigraphic permeability within dipping sequences is likely to be secondarily important.
7. No active fluid venting has yet been recognized over the frontal accretionary wedge, but the presence of a widespread BSR, extensive protothrust zone, and two unconfirmed sites of possible previous fluid expulsion, indicates that the frontal wedge is actively dewatering. There are presently no constraints however on the relative fluid flux between the frontal wedge and the active mid-slope fluid seeps.

Acknowledgments

We thank the crew and officers of *RV SONNE* cruise SO191, and the multiple *RV TANGAROA* voyages that contributed data to this study. The New Zealand Ministry for Economic Development provided us access to the CM05 seismic dataset. PB and GL were funded by NZ FRST research contracts CO1X0203 and CO1X0702. SH was funded by NZ FRST contract CO5X0302. The 'New Vents' project including the cruise SO191 was funded by the German Ministry of Education and Research (BMBF). JM was partly funded by a Tertiary Education Top Achiever Award. GC was funded through the Royal Society of New Zealand Marsden Grant contract GNS0403. The distribution of active faults on land was provided by GNS Science. We thank John Mitchell, Steve Wilcox and Peter Gerring for assistance with data acquisition, Claire Castellazzi for processing and display of seismic data, and Rob Funnell for discussion of heat flow. The *RV TANGAROA* seismic and EM300 multibeam dataset used here from the southern Poverty Bay margin were acquired for a related study by Keith Lewis. We appreciate constructive reviews of the manuscript by Andy Nicol and Chris Goldfinger.

References

Arron, E.S., Lewis, K.B., 1992. Mahia, 2nd Edition, N. Z. Oceanographic Institute Chart, Coastal Series, 1:200 000. Department of Scientific and Industrial Research, Wellington, New Zealand.

Ballance, P.F., 1976. Evolution of the Upper Cenozoic magmatic arc and plate boundary in northern New Zealand. Earth Planet. Sci. Lett. 28, 356–370.

Bangs, N.L., Shipley, T.H., Moore, J.C., Moore, G.F., 1999. Fluid accumulation and channeling along the northern Barbados décollement thrust. J. Geophys. Res. 104, 20,399–20,414.

Bangs, N.L., Shipley, T.H., Gulick, S., Moore, G., Kuomoto, S., Nakamura, Y., 2004. Evolution of the Nankai Trough décollement from the trench into the seismogenic zone: inferences from three-dimensional seismic reflection imaging. Geology 32, 273–276.

Barker, D.H.N., Sutherland, R., Henrys, S., Bannister, S., 2009. Geometry of the Hikurangi subduction thrust and upper plate, North Island, New Zealand. Geochem. Geophys. Geosyst. 10, Q02007. doi:10.1029/2008GC002153.

Barnes, P.M., Audru, J.-C., 1999. Quaternary faulting in the offshore Flaxbourne and southern Wairarapa basins, southern Cook Strait, New Zealand. N. Z. J. Geol. Geophys. 42, 349–367.

Barnes, P.M., Korsch, R.J., 1991. Melange and related structures in Torlesse accretionary wedge, Wairarapa, New Zealand. N. Z. J. Geol. Geophys. 34, 517–532.

Barnes, P.M., Mercier de Lépinay, B., 1997. Rates and mechanics of rapid frontal accretion along the very obliquely convergent southern Hikurangi margin, New Zealand. J. Geophys. Res. 102, 24 931–24 952.

Barnes, P.M., Nicol, A., 2004. Formation of an active thrust triangle zone associated with structural inversion in subducting setting, eastern New Zealand. Tectonics 23 (1), TC1015.

Barnes, P.M., Mercier de Lépinay, B., Collot, J.-Y., Delteil, J., Audru, J.-C., 1998a. Strain partitioning in the transition area between oblique subduction and continental collision, Hikurangi margin, New Zealand. Tectonics 17, 534–557.

Barnes, P.M., Mercier de Lépinay, B., Collot, J.-Y., Delteil, J., Audru, J.-C., and GeodyNZ team, 1998b. South Hikurangi GeodyNZ swath maps: depths, texture and geological interpretation. 1:500,000., N.Z. Oceanogr. Inst. Chart, Miscellaneous Series 75. National Institute of Water and Atmospheric Research, Wellington.

Barnes, P.M., Nicol, A., Harrison, T., 2002. Late Cenozoic evolution and earthquake potential of an active listric thrust complex above the Hikurangi subduction zone, New Zealand. Geol. Soc. Am. Bull. 114, 1379–1405.

Beavan, J., Tregoning, P., Bevis, M., Kato, T., Meertens, C., 2002. Motion and rigidity of the Pacific Plate and implications for plate boundary deformation. J. Geophys. Res. 107, 2261 (ETG 19).

Brown, K.M., Kopf, A., Underwood, M.B., Weinberger, J.L., 2003. Compositional and fluid pressure controls on the state of stress on the Nankai subduction thrust: a weak plate boundary. Earth Planet. Sci. Lett. 214, 589–603.

Bryne, T., Fisher, D., 1990. Evidence for a weak and overpressured décollement beneath sediment-dominated accretionary prisms. J. Geophys. Res. 95, 9081–9097.

Campbell, K.A., Francis, D.A., Collins, M., Gregory, M.R., Nelson, C.S., Greinert, J., Aharon, P., 2008. ?Hyrdocarbon seep-carbonates of a Miocene forearc (East Coast Basin), North Island, New Zealand. Sediment. Geol. 204, 83–105.

Collot, J.-Y., Delteil, J., Lewis, K.B., Davy, B., Lamarche, G., Audru, J.-C., Barnes, P.M., Chanier, F., Chaumillon, E., Lallemand, S., Mercier de Lépinay, B., Orpin, A.R., Pelletier, B., Sosson, M., Toussaint, B., Uruski, C., 1996. From oblique subduction to intra-continental transpression: structures of the southern Kermadec–Hikurangi margin from multibeam bathymetry, side-scan sonar and seismic reflection. Mar. Geophys. Res. 18, 357–381.

Collot, J.-Y., Lewis, K.B., Lamarche, G., Lallemand, S., 2001. The giant Ruatoria debris avalanche on the northern Hikurangi margin, New Zealand; results of oblique seamount subduction. J. Geophys. Res. 106, 19271–19297.

Cowan, D.S., 1982. Structural stles in Mesozoic and Cenozoic mélanges in the Western Cordellia of North America. Geol. Soc. Am. Bull. 96, 451–462.

Crutchley, G.J., Pecher, I.A., Gorman, A.R., Henrys, S.A., Greinert, J., 2010. Seismic imaging of gas conduits beneath seafloor seep sites in a shallow marine gas hydrate province, Hikurangi Margin, New Zealand. Mar. Geol. 272, 114–126 (this issue).

Darby, D., 2002. Seal properties, overpressure and stress in the Taranaki and East Coast Basins, New Zealand. New Zealand Petroleum Conference Proceedings. Ministry of Commerce, Wellington.

Darby, D., Funnell, R., Uruski, C., Field, B., 2000. Patterns of fluid flow in the East Coast Basin. New Zealand Petroleum Conference Proceedings. Ministry of Commerce, Wellington.

Davy, B., Wood, R., 1994. Gravity and magnetic modelling of the Hikurangi Plateau. Mar. Geol. 118, 139–151.

Davy, B.R., Hoernle, K., Werner, R., 2008. The Hikurangi Plateau — crustal structure, rifted formation and Gondwana subduction history. Geochem. Geophys. Geosyst. 9, Q07004. doi:10.1029/2007GC001855.

Davey, F.J., Lewis, K.B., Childs, J., Hampton, M., 1986a. Convergent margin off the east coast of North Island, New Zealand, Parts I and II. In: von Huene, R.E. (Ed.), Seismic Images of Modern Convergent Margin Structure. Am. Assoc. Pet. Geol. Stud. Geol., vol. 26, pp. 49–53.

Davey, F.J., Hampton, M., Childs, J., Fisher, M.A., Lewis, K.B., Pettinga, J.R., 1986b. Structure of a growing accretionary prism, Hikurangi margin, New Zealand. Geology 14, 663–666.

Davies, E.J., Frederick, J.B., Leask, W.L., Williams, T.J., 2000. East Coast drilling results. New Zealand Petroleum Conference Proceedings. Ministry of Commerce, Wellington.

Davis, D., Suppe, J., Dahlen, F.A., 1983. Mechanics of fold and thrust belts and accretionary wedges. J. Geophys. Res. 88, 1153–1172.

Dixon, T.H., Moore, J.C., 2007. The seismogenic zone of subduction thrust faults: introduction. In: Dixon, T.H., Moore, J.C. (Eds.), The Seismogenic Zone of Subduction Thrust Faults. Columbia University Press, New York, pp. 2–14.

Dominguez, S., Lallemand, S.E., Malavieille, J., von Huene, R., 1998. Upper plate deformation associated with seamount subduction. Tectonophysics 293, 207–224.

Ellis, S., Pecher, I., Kukowski, N., Xu, W., Henrys, S., Greinert, J., 2010. Testing proposed mechanisms for seafloor weakening at the top of gas hydrate stability, Rock Garden, New Zealand. Mar. Geol. 272, 127–140 (this issue).

Ernst, W.G., 1990. Thermobarometric and fluid expulsion history of subduction zones. J. Geophys. Res. 95, 9047–9053.

Faure, K., Greinert, J., Pecher, I.A., Graham, I.J., Massoth, G.J., Ronde, C.E.J.D., Wright, I.C., Baker, E.T., Olson, E.J., 2006. Methane seepage and its relation to slumping and gas hydrate at the Hikurangi Margin, New Zealand. N. Z. J. Geol. Geophys. 49, 503–516.

Faure, K., Greinert, J., von Deimling, J.S., McGinnis, D.F., Kipfer, R., Linke, P., 2010. Methane seepage along the Hikurangi Margin of New Zealand: Geochemical and physical data from the water column, sea surface and atmosphere. Mar. Geol. 272, 170–188 (this issue).

Field, B.D., Uruski, C.I., et al., 1997. Cretaceous–Cenozoic Geology and Petroleum Systems of the East Coast Region, New Zealand. Institute of Geological & Nuclear Sciences Monograph, vol. 19. Institute of Geological & Nuclear Sciences Ltd, Lower Hutt, New Zealand. 301 pp.

Frederik, J.B., 2004. East Coast hydrocarbon potential — Tawatawa prospect, offshore Wairarapa shelf. New Zealand Petroleum Conference Proceedings. Ministry of Commerce, Wellington.

Garlick, R., Mitchell, J.S., 2002. Turnagain Bathymetry, 3rd Edition. NIWA Chart, Coastal Series, 1:200 000. National Institute of Water and Atmospheric Research Ltd, Wellington, New Zealand.

Gee, M.J.R., Uy, H.S., Warren, J., Morley, C.K., Lambaise, J.J., 2007. The Brunei slide: a giant submarine landslide on the North West Borneo Margin revealed by 3D seismic data. Mar. Geol. 246, 9–23.

Greinert, J., Lewis, K., Bialas, J., Pecher, I., Rowden, A., Linke, P., De Batist, M., Bowden, D., Suess, E., 2010. Methane seepage along the Hikurangi Margin, New Zealand: review of studies in 2006 and 2007 and new evidence from visual, bathymetric and hydroacoustic investigations. Mar. Geol. 272, 6–25 (this issue).

Haeckel, M., Sommer, S., Linke, P.: this volume. Porewater geochemistry and methane fluxes of cold seeps at the Hikurangi Margin, offshore New Zealand. Mar. Geol.

Henry, P., Le Pichon, X., Lallemant, S., Foucher, J.-P., Westbrook, G., Hobart, M., 1990. Mud volcano field seaward of the Barbados accretionary complex: a deep-towed side-scan sonar survey. J. Geophys. Res. 95, 8917–8930.

Henrys, S.A., Ellis, S., Uruski, C., 2003. Conductive heat flow variations from bottom simulating reflectors on the Hikurangi margin, New Zealand. Geophys. Res. Lett. 30. doi:10.1029/2002GL015772.

Henrys, S., Reyners, M., Pecher, I., Bannister, S., Nishimura, Y., Maslen, G., 2006. Kinking of the subducting slab by escalator normal faulting beneath the North Island of New Zealand. Geology 34, 777–780.

Henrys, S.A., Woodward, D., Pecher, I.A., in press. Variation of bottom-simulating reflector (BSR) strength in a high-flux methane province, Hikurangi margin, New Zealand. Am. Assoc. Pet. Geol. Memoirs.

Holt, W.E., Haines, A.J., 1995. The kinematics of northern South Island, New Zealand, determined from geological strain rates. J. Geophys. Res. 100, 17991–18010.

Huhnerbach, V., Masson, D.G., Bohrmann, G., Bull, J.M., Weinrebe, W., 2005. Deformation and submarine landsliding caused by seamount subduction beneath the Costa Rica continental margin — new insights from high-resolution sidescan sonar data. In: Hodgson, D.M., Flint, S.S. (Eds.), Submarine Slope Systems: Processes and Products. Geol. Soc. Lond. Spec. publ., vol. 244, pp. 195–205.

Jones, A.T., Greinert, J., Bowden, D., Klaucke, I., Petersen, J., Netzeband, G., Weinrebe, W., 2010. Acoustic and visual characterisation of methane-rich seabed seeps at Omakere Ridge on the Hikurangi Margin, New Zealand. Mar. Geol. 272, 154–169 (this issue).

Karig, D.E., Lundberg, N., 1990. Deformation bands from the toe of the Nankai accretionary prism. J. Geophys. Res. 95, 9099–9109.

Katz, H.R., 1981. Probable gas hydrate in continental slope east of the North Island, New Zealand. J. Pet. Geol. 3, 315–324.

Klaucke, I., Weinrebe, W., Petersen, C.J., Bowden, D., 2010. Temporal variability of gas seeps offshore New Zealand: multi-frequency geoacoustic imaging of the Wairarapa area, Hikurangi margin. Mar. Geol. 272, 49–58 (this issue).

Kvenvolden, K.A., 1993. Gas hydrates — geological perspective and global change. Rev. Geophys. Space Phys. 31, 173–187.

Kvenvolden, K.A., Pettinga, R., 1989. Hydrocarbon gas seeps of the convergent Hikurangi margin, North Island, New Zealand. Mar. Pet. Geol. 6, 2–8.

Kulm, L.D., Suess, E., 1990. Relationship between carbonate deposits and fluid venting: Oregon accretionary prism. J. Geophys. Res. 95, 8899–8916.

Lallemand, S., Schnurle, P., Malavieille, J., 1994. Coulomb theory applied to accretionary and nonaccretionary wedges: possible causes for tectonic erosion and/or frontal accretion. J. Geophys. Res. 99, 12033–12055.

Lamb, S., 2006. Shear stresses on megathrusts: implications for mountain-building behind subduction zones. J. Geophys. Res. 111, B07401. doi:10.1029/2005JB003916.

Langseth, M.G., Moore, J.C., 1990. Introduction to special section on the role of fluids in sediment accretion, deformation, diagenesis, and metamorphism in subduction zones. J. Geophys. Res. 95, 8737–8742.

LePichon, X., Henry, P., Lallement, S., 1990. Water flow in the Barbados accretionary complex. J. Geophys. Res. 95, 8945–8968.

Lewis, K.B., 1973. Erosion and deposition on a tilting continental shelf during Quaternary oscillations of sea level. N. Z. J. Geol. Geophys. 16, 281–301.

Lewis, K.B., Barnes, P.M., 1999. Kaikoura Canyon, New Zealand; active conduit from near-shore sediment zones to a trench-axis channel. Mar. Geol. 162, 39–69.

Lewis, K.B., Marshall, B.A., 1996. Seep faunas and other indictors of methane-rich dewatering on the New Zealand convergent margins. N. Z. J. Geol. Geophys. 39, 181–200.

Lewis, K.B., Pettinga, J.R., 1993. The emerging, imbricate frontal wedge of the Hikurangi margin. In: Balance, P.F. (Ed.), South Pacific Sedimentary Basins. Sedimentary Basins of the World 2, Basins of the Southwest Pacific. Elsevier, Amsterdam, pp. 225–250.

Lewis, K.B., Collot, J.-Y., Davy, B.W., Delteil, L., Lallemand, S.E., Uruski, C.I. and GeodyNZ team, 1997. North Hikurangi GeodyNZ swath maps: depth, texture and geological interpretation. NIWA chart miscellaneous series vol. 72. National Institute of Water & Atmospheric Research, Wellington.

Lewis, K.B., Collot, J.-Y., Lallemand, S.E., 1998. The dammed Hikurangi Trough: a channel-fed trench blocked by subducting seamounts and their wake avalanches (New Zealand–France GeodyNZ Project). Bas. Res. 10, 441–468.

Lewis, K.B., Barnes, P.M., Collot, J.-Y., Mercier de Lépinay, B., Delteil, J., and GeodyNZ team, 1999. Central Hikurangi GeodyNZ swath maps: depth, texture and geological interpretation. NIWA chart miscellaneous series 77. National Institute of Water & Atmospheric Research, Wellington.

Lewis, K.B., Lallemand, S., Carter, L., 2004. Collapse in a Quaternary shelf basin off East Cape, New Zealand: evidence for the passage of a subducted seamount inboard of the Ruatoria giant avalanche. N. Z. J. Geol. Geophys. 47, 415–429.

Maltman, A.J., Byrne, T., Karig, D.E., Lallemant, S., 1993. Deformation at the toe of an active accretionary prism: synopsis of results from ODP Leg 131, Nankai, SW Japan. J. Struct. Geol. 15, 949–964.

McCaffrey, R., Wallace, L.M., Beavan, J., 2008. Slow slip events, temperature, and interseismic coupling at the Hikurangi subduction zone, New Zealand. Nat. Geosci. 1, 316–320.

Mitchell, J.S., 1988. Palliser Bathymetry 2nd Edition, N. Z. Oceanographic Institute Chart, Coastal Series, 1:200 000. Department of Scientific and Industrial Research, Wellington, New Zealand.

Moore, J.C., 1989. Tectonics and hydrogeology of accretionary prisms: role of the decollement zone. J. Struct. Geol. 11, 95–106.

Moore, J.C., Byrne, T., 1987. Thickening of fault zones: a mechanism of melange formation in accretionary sediments. Geology 15, 1040–1043.

Moore, J.C., Saffer, D., 2001. Updip limit of the seismogenic zone beneath the accretionary prism of southwest Japan; an effect of diagenetic to low-grade metamorphic processes and increasing effective stress. Geology 29, 183–186.

Moore, J.C., Vrolijk, P., 1992. Fluids in accretionary prisms. Rev. Geophys. 30, 113–135.
Moore, J.C., Wheeler, R.W., 1978. Structural fabric of a mélange, Kodiac Isalnds, Alaska. Am. J. Sci. 278, 739–765.
Moore, J.C., Roeske, S., Lundberg, N., Schoonmaker, J., Cowan, D.S., Gonzales, E., Lucas, S.E., 1986. Scaly fabrics from Deep Sea Drilling Project cores from forearcs. In: Moore, J.C. (Ed.), Structural Fabrics in Deep Sea Drilling Project Cores. Mem. Geol. Soc. Am., vol. 166, pp. 55–74.
Moore, G.F., Shipley, T.H., Stoffa, P.L., Karig, D.E., Taira, A., Kuramoto, S., Tokuyama, H., Suyehiro, K., 1990. Structure of the Nankai Trough accretionary zone from multichannel seismic reflection data. J. Geophys. Res. 95, 8753–8765.
Moore, J.C., Moore, G.F., Cochrane, G.R., Tobin, H.J., 1995. Negative-polarity seismic reflections along faults of the Oregon accretionary prism: indicators of overpressuring. J. Geophys. Res. 100, 12895–12906.
Moore, G.F., Bangs, G.F., Taira, A., Kuramoto, S., Pangborn, E., Tobin, H.J., 2007. Science 318, 1128–1131.
Morgan, J.K., Karig, D.E., 1995. Decollement processes at the Nankai accretionary margin, southeast Japan: propagation, deformation, and dewatering. J. Geophys. Res. 100, 15221–15231.
Morgan, J.K., Sunderland, E.B., Ask, M.V.S., 2007. Deformation and mechanical strength of sediments at the Nankai subduction zone: implications for prism evolution and décollement initiation and propagation. In: Dixon, T.H., Moore, J.C. (Eds.), The Seismogenic Zone of Subduction Thrust Faults. Columbia University Press, New York, pp. 210–247.
Mountjoy, J., Barnes, P., Pettinga, J., 2009. Morphostructure of submarine canyons on an active margin: Cook Strait Canyon system, New Zealand. Mar. Geol. 260, 45–68. doi:10.1016/j.margeo.2009.01.006.
Multiwave, 2005. 05CM 2D Seismic Survey, Offshore East Coast — North Island. New Zealand unpublished openfile petroleum report 3136. Ministry of Economic Development, Wellington.
Naudts, L., Greinert, J., Poort, J., Belza, J., Vangampelaere, E., Boone, D., Linke, P., Henriet, J.-P., De Batist, M., 2010. Active venting sites on the gas-hydrate-bearing Hikurangi Margin, Off New Zealand: diffusive versus bubble-released methane. Mar. Geol. 272, 233–250 (this issue).
Netzeband, G.L., Krabbenhoeft, A., Zillmer, M., Petersen, C.J., Papenberg, C., Bialas, J., 2010. The structures beneath submarine methane seeps: Seismic evidence from Opouawe Bank, Hikurangi Margin, New Zealand. Mar. Geol. 272, 57–70 (this issue).
Nicol, A., Mazengarb, C., Chanier, F., Rait, G., Uruski, C., Wallace, L., 2007. Tectonic evolution of the Hikurangi subduction margin, New Zealand, since Oligocene. Tectonics 26. doi:10.1029/2006TC002090.
Nimblett, J., Ruppel, C., 2003. Permeability evolution during the formation of gas hydrates in marine sediments. J. Geophys. Res. 108. doi:10.1029/2001JB001650.
Paquet, F. 2008. Morphostructural evolution of active subduction margins: the example of the Hawke bay Forearc Basin, New Zealand. PhD Thesis, Universite de Rennes 1, Rennes, France and University of Canterbury, Christchurch, New Zealand, 253 pp.
Paquet, F., Proust, J.-N., Barnes, P.M., Pettinga, J., 2009. Inner forearc sequence architecture in response to climate and tectonic forcing since 150 Ka: Hawke's Bay, New Zealand. J. Sediment. Res. 79, 97–124. doi:10.2110/jsr.2009.019.
Pecher, I.A., 2002. Gas hydrates on the brink. Nature (News and views) 420, 622–623.
Pecher, I.A., Henrys, S.A., Zhu, H., 2004. Seismic images of gas conduits beneath vents and gas hydrates on Ritchie Ridge, Hikurangi Margin, New Zealand. N. Z. J. Geol. Geophys. 47, 275–279.
Pecher, I.A., Henrys, S.A., Ellis, S., Chiswell, S.M., Kukowski, N., 2005. Erosion of the seafloor at the top of the gas hydrate stability zone on the Hikurangi Margin, New Zealand. Geophys. Res. Lett. 32, L24603.
Pecher, I.A., Henrys, S.A., Wood, W.T., Kukowski, N., Crutchley, G.J., Fohrmann, M., Kilner, J., Senger, K., Gorman, A.R., Coffin, R.B., Greinert, J., Faure, K., 2010. Focused fluid flow on the Hikurangi Margin, New Zealand - evidence from possible local upwarping of the base of gas hydrate stability. Mar. Geol. 272, 99–113 (this issue).
PettingaJ.R., J.R., 1982. Upper Cenozoic structural history, coastal southern Hawke's Bay, New Zealand. N. Z. J. Geol. Geophys. 25, 149–191.
Pettinga, J.R., 2003. Mud volcano eruption within the emergent accretionary Hikurangi margin, southern Hawke's Bay, New Zealand. N. Z. J. Geol. Geophys. 46, 107–121.
Platt, J., 1990. Thrust mechanics in highly overpressured accretionary wedges. J. Geophys. Res. 95, 9025–9034.
Ridd, M.F., 1970. Mud volcanoes in New Zealand. Am. Assoc. Pet. Geol. Bull. 54, 601–616.
Rait, G., Chanier, F., Waters, D.W., 1991. Landward- and seaward-directed thrusting accompanying the onset of subduction beneath New Zealand. Geology 19, 230–233.
Saffer, D.M., 2003. Pore pressure development and progressive dewatering in underthrust sediments at the Costa Rican subduction margin: comparison with northern Barbados and Nankai. J. Geophys. Res. 108, 2261. doi:10.1029/2002JB001787.
Saffer, D.M., 2007. Pore pressure within underthrust sediment in subduction zones. In: Dixon, T.H., Moore, J.C. (Eds.), The Seismogenic Zone of Subduction Thrust Faults. Columbia University Press, New York, pp. 148–170.
Saffer, D.M., Bekins, B.A., 2002. Hydrologic controls on the mechanics and morphology of accretionary wedges and thrust belts. Geology 30, 271–274.
Schwalenberg, K., Wood, W., Pecher, I., Hamden, L., Henrys, S., Jegen, M., Coffin, R.B., 2010. Preliminary interpretation of CSEM, heatflow, seismic, and geochemical data for gas hydrate distribution across the Porangahau Ridge, New Zealand. Mar. Geol. 272, 89–98 (this issue).
SibsonR.H., R.H., 1992. Fault-valve behaviour and the hydrostatic–lithostatic fluid pressure interface. Earth Sci. Rev. 32, 141–144.
Sibson, R.H., Roland, J., 2003. Stress, fluid pressure and structural permeability in seismogenic crust, North Island, New Zealand. Geophys. J. Int. 154, 584–594.
Taira, A., Hill, I., Firth, J., Berner, U., Bruckmann, W., Bryne, T., Chabernaud, T., Fisher, A., Foucher, J.-P., Gamo, T., Gieskes, J., Hyndman, R., Karig, D., Kastner, M., Kaot, Y., Lallemant, S., Lu, R., Maltman, A., Moore, G., Moran, K., Olaffson, G., Owens, W., Pickering, K., Siena, F., Taylor, E., Underwood, M., Wilkinson, C., Yamano, M., Zhang, J., 1992. Sediment deformation and hydrogeology of the Nankai Trough accretionary prism: synthesis of shipboard results of ODP Leg 131. Earth Planet. Sci. Lett. 109, 431–450.
Townend, J., 1997a. Subducting a sponge: minimum estimates of the fluid budget of the Hikurangi margin accretionary prism. Geol. Soc. N.Z. Newslett. 112, 14–16.
Townend, J., 1997b. Estimates of conductive heat flow through bottom-simulating reflectors on the Hikurangi and southwest Fiordland continental margins, New Zealand. Mar. Geol. 141, 209–220.
Tobin, H.J., Moore, J.C., Moore, G.F., 1994. Fluid pressure in the frontal thrust of the Oregon accretionary prism: experimental constraints. Geology 22, 979–982.
Trehu, A.M., Torres, M.E., Moore, G.F., Suess, E., Bohrmann, G., 1999. Temporal and spatial evolution of a gas hydrate-bearing accretionary ridge on the Oregon continental margin. Geology 27, 939–942.
Uruski, C., Field, B., Sykes, R., Funnell, R., Darby, D., 2004. Is the offshore East Coast Basin an accessible source of gas? New Zealand Petroleum Conference Proceedings. Ministry of Commerce, Wellington.
Von Huene, R., Lallemand, S., 1990. Tectonic erosion along the Japan and Peru convergent margins. Geol. Soc. Am. Bull. 102, 704–720.
von Huene, R., Scholl, D.W., 1991. Observations at convergent margins concerning sediment subduction, subduction erosion, and the growth of continental crust. Rev. Geophys. 29, 279–316.
Vrolijk, P., 1990. On the mechanical role of smectite in subduction zones. Geology 18, 703–707.
Wallace, L.M., Beavan, J., McCaffrey, R., Darby, D., 2004. Subduction zone coupling and tectonic block rotation in the North Island, New Zealand. J. Geophys. Res. 109. doi:10.1029/2004JB003241.
Wood, R., Davy, B., 1994. The Hikurangi Plateau. Mar. Geol. 118, 153–173.